Environmental Science and Pollution Research (2022) 29:69402–69423
https://doi.org/10.1007/s11356-022-20411-x

RESEARCH ARTICLE

Experimental investigations and the modeling approach for CO_2 solubility in aqueous blended amine systems of monoethanolamine, 2-amino-2-methyl-1-propanol, and 2-(butylamino)ethanol

Tianci Li[1] · Congning Yang[1] · Puttipong Tantikhajorngosol[1] · Teerawat Sema[1,2] · Huancong Shi[3,4] · Paitoon Tontiwachwuthikul[1]

Received: 14 October 2021 / Accepted: 19 April 2022 / Published online: 14 May 2022

Abstract
In this work, new CO_2 solubility data on three types of aqueous amine blends were reported to complement existing databases. The experiments were conducted at temperatures of 313 K (absorption condition) and 363 K (desorption condition). The effect of the MEA concentration on the CO_2 solubility in several amine blends at low CO_2 partial pressure (8 to 50.65 kPa) were studied in this work, including 0.1, 0.3, 0.5 mol/L MEA + 2 mol/L AMP; 0.1, 0.3, 0.5 mol/L MEA + 2 mol/L BEA; and 0.1, 0.3, 0.5 mol/L MEA + 1, 2 mol/L AMP + 1, 2 mol/L BEA. Besides, an additional group of equilibrium CO_2 solubility data were conducted at 298 K in order to estimate the heat of CO_2 absorption of the blended solvents at a temperature range from 298 to 313 K. A new simplified Kent-Eisenberg model was developed for the predictions of blended solvents, and a multilayer neural network model with Levenberg–Marquardt backpropagation algorithm was developed upon five hundred reliable published experimental data. The predictions from two methods are both in good agreement with the experimental CO_2 solubility data.

Keywords CO_2 solubility · Amine blends · Machine learning · CO_2 capture · Kent-Eisenberg · Thermodynamics

Introduction

In recent years, people are experiencing and facing substantial challenges from nature, such as extreme cold weather, new virus, wildfires, and flooding in coastal areas. These significant impacts of the ecosystem are all linked to climate change. Several national governments and international organizations have announced their carbon neutral target in the next few decades. However, fossil fuels are still the largest energy contributors throughout the world (International Energy Agency 2020). This situation would not be changed rapidly particularly in the developing countries. Renewable energy sources are ideally cleaner energy contributors than combustible fuels for power generations, but it is not convincing that they could completely substitute the fossil fuels shortly due to the limited energy generation capacity and high costs. Hence, several countries seek their own strategies to achieve energy transition. The goal is to gradually replace the demand of coal and oil by low carbon fuels or sustainable combustible materials, such as natural gas and biomass. The utilizations of these energy sources could conceptually reduce a certain amount of direct carbon emissions rapidly, but their total carbon emissions cannot be overlooked from long-term observation. Additionally, CO_2 which is released from the industry such as cement plants and refineries must be accounted as a considerable emission source. There is currently no efficient alternative solution to substitute these products from the industry. Carbon capture technologies

Responsible Editor: Santiago V. Luis

✉ Huancong Shi
hcshi@usst.edu.cn

✉ Paitoon Tontiwachwuthikul
paitoon@uregina.ca

[1] Clean Energy Technologies Research Institute (CETRI), University of Regina, Regina, SK, Canada

[2] Department of Chemical Technology, Faculty of Science, Chulalongkorn University, Bangkok, Thailand

[3] Department of Environmental Science and Engineering, University of Shanghai for Science and Technology, Shanghai 200093, People's Republic of China

[4] Huzhou Institute of Zhejiang University, Huzhou, Zhejiang 313000, People's Republic of China

thus become the logical path to reduce the carbon emission for the purpose of decarbonization.

The chemical absorption process is a mature technology applied in CO_2 capture. Monoethanolamine (MEA) has been widely studied as the main solvent for the conventional amine-based chemical CO_2 absorption process. It is also known that the amine-based chemical absorption process highly relies on the amine reaction with CO_2 and forming to the zwitterions, which is also used to determine the absorption rate. MEA is a typical primary amine which provides a fast reaction rate with CO_2, but the low absorption capacity and high desorption energy demand are its main drawbacks leading to high operating costs. In the past few years, extensive publications discovered the benefits and limitations of various single amines. Based on the single-amine solvent, blending amine solvents is a promising idea to improve the absorption and desorption performance. Therefore, the development of highly efficient solvents is gradually becoming a strategy for the further development of carbon capture technology. The selection of proper amine could be one of the major fundamental steps for the process. Recently, there are two common blending approaches based on using MEA: (i) considering MEA as a major base solvent, blending one or more carbonate formation solvent(s) or the amine(s) with larger CO_2 absorption capacity, such as sterically hindered amines, poly amines, and secondary amines, and (ii) considering MEA as a promoter, blending a small amount of MEA into secondary amines (i.e., diethanolamine and 2-(butylamino) ethanol) or related blend amine solvents to achieve the "coordinative effect" (Shi et al. 2021a, b). On the other hand, MEA has become a major solvent applied to commercial-scale CO_2 capture because of its great CO_2 absorption rate. Thus, the relative mature product supply chain of MEA can directly lead to its superiority of price and technology in the industry. Therefore, blending MEA with advanced solvent(s) is beneficial if the solvent is further commercialized.

2-Amino-2-methyl-1-propanol (AMP) is a typical sterically hindered amine, which is the simplest hindered form of MEA (Tong et al. 2013). The CO_2 solubility in aqueous AMP has been investigated extensively from sufficient published studies (Tontiwachwuthikul et al. 1991; Jane and Li 1997; Kundu et al. 2003; Li and Chang 1995). They affirmed that AMP provides large CO_2 absorption capacity with moderate reaction kinetics attributed to the formation of carbamate during the direct reaction between AMP and CO_2. However, its reaction kinetics with CO_2 is weaker than using MEA; hence, the benefits of large CO_2 absorption capacity could not be exhibited well at low-pressure operations (Tong et al. 2013). In contrast, for 2-(butylamino) ethanol) (BEA) which is a secondary amine, only a few researchers studied the CO_2 absorption capacity using aqueous single-BEA solvent (Hwang et al. 2017; Narku-Tetteh et al. 2017a, b). Recently, the majority of the studies associated with BEA have been staying at the laboratory stage. In terms of laboratory applications, BEA is more expensive than MEA, but cheaper than AMP. However, the further practical commercial-scale applications should also consider various direct and indirect operating costs, such as energy costs, maintenance costs, and waste disposal. BEA is a promising secondary amine; it has higher desorption efficiency compared to MEA and other typical secondary amines including 2-(ethylamino)ethanol (EAE) and 2-(methylamino)ethanol (MAE) (Ping et al. 2020). Secondary alkanolamines tend to provide larger CO_2 absorption capacity than MEA due to the formation of bicarbonate and exhibit weaker carbamate stability (Hwang et al. 2017). Despite that Narku-Tettech et al. (2017) found the excellent CO_2 absorption/desorption performance using several BEA-based solvent blends, including BEA + AMP (2 mol/L + 2 mol/L and 2.5 mol/L + 2.5 mol/L) and MEA + BEA + AMP (1 mol/L + 2 mol/L + 2 mol/L), they did not extensively investigate the CO_2 solubility with various concentration ratios at different pressures and temperatures. The lack of solubility data leads to a knowledge gap, so it is essential to investigate the CO_2 solubility at a wider temperature range. In fact, CO_2 solubility is an important property which reflects the maximum volume (or mass) of CO_2 which can be absorbed into the given amount of solvent. In other words, CO_2 solubility represents the absorption capacity. Generally, CO_2 has a lower tendency to be trapped in the solvent when near the equilibrium; thus, the solvent with greater CO_2 solubility is more beneficial. Consequently, a promising solvent candidate should absorb more CO_2 than the benchmark solvent MEA at the same operating conditions. CO_2 solubility can be considered as a key factor influencing both absorption and desorption performance. It is known that CO_2 solubility is highly influenced by the operating temperature. It is increased by reducing the temperature. In this solvent screening work, the low operating temperature (313 K) and the high operating temperature (363 K) represent the absorption and the desorption operating environment, respectively. In this case, a solvent with higher CO_2 solubility in low operating temperature and lower CO_2 solubility in high operating temperature should be considered as a potential candidate. Besides, Shi et al. (2021a, b) explained the coordinative effects by adding a small amount of MEA into the BEA/AMP blends to achieve an enhanced CO_2 absorption performance. In the meantime, there was no significant negative impact of desorption performance appeared when they added the small amount of MEA into the blends compared to the tri-solvent blends that contain a higher concentration of MEA. The coordinative effects were achieved through the proton transfer within primary amine and secondary amine for both absorption and desorption processes. They also proved that adding a small amount (0.1 to 0.5 mol/L) of MEA into BEA/AMP

(2 + 2 mol/L) could even exhibit better desorption performance than the bi-solvent BEA/AMP (2 + 2 mol/L). This phenomenon is resulted by the small amount of MEA, which could facilitate $BEAH^+$ regeneration, increase CO_2 capture performance, and reduce heat duty requirement. Based on the achievement from the previous study (Shi et al. 2021a, b; Shi et al. 2021a, b), this research is an extended study for investigating equilibrium CO_2 solubility and the heat of CO_2 absorption in several bi-solvent and tri-solvent blends in order to comprehensively evaluate the CO_2 capture performances. The solvent blends presented in this research are MEA + AMP (0.1, 0.3, 0.5 mol/L + 2 mol/L), MEA + BEA (0.1, 0.3, 0.5 mol/L + 2 mol/L), and MEA + AMP + BEA (0.1, 0.3, 0.5 mol/L + 1, 2 mol/L + 1, 2 mol/L).

In this work, an artificial neural network (ANN) model and a Kent-Eisenberg model are presented for the prediction of the CO_2 solubility. The Kent-Eisenberg (KE) model is firstly proposed by Kent and Eisenberg (1976); it is a typical non-rigorous empirical model which can be applied to predict the equilibrium data in amine systems using apparent equilibrium constants. This model is a simplified thermodynamic model, which assumes to ignore the system non-ideality. Thus, all fugacity coefficients and activity coefficients are supposed to be unity (Hwang et al. 2016; Austgen et al. 1991; Li and Shen 1993; Hu and Chakma 1990). ANN is a typical machine learning approach widely applied in industry nowadays. ANNs are multifaceted tools that imitate the human brain to process the complex data sets through linear or nonlinear processes (Sipocz et al. 2016). ANNs have been extensively used in the CO_2 capture process to predict mass transfer performance and various physical and chemical properties of the solvent (Liu et al. 2019; Fu et al. 2013). For the predictions of CO_2 solubility, several researchers have confirmed that an optimal ANN model could provide closer predictions to the experimental data due to its comprehensive experimental database compared to other prediction tools, such as simulation tools (e.g., Aspen Plus, ProMax) and common thermodynamic models (Liu et al. 2017a, b; Li et al. 2017, 2021). The proposed architectures of ANN models are trained and validated by using sufficient published experimental data and new experimental data from this study.

Unlike thermodynamic models, ANN is a mathematical tool to process the data. Hence, there is no comparability of the computational mechanism between two methods. As reliable prediction tools, the accuracy of their prediction results could potentially reflect their benefits and limitations. Thereby, the comparisons of experimental results and their prediction results are discussed in this research. Also, the reliability and accuracy of ANN predictions were studied by comparing with the prediction accuracy using other conventional thermodynamic models, including the SAFT expression of Huang and Radosz (SAFT-HR) and the SAFT expression of the perturbed-chain statistical method (PC-SAFT). It should be noticed that the prediction accuracy was determined by comparing experimental results to modeling predictions; it cannot be directly estimated by comparing the prediction results from different models without experimental results.

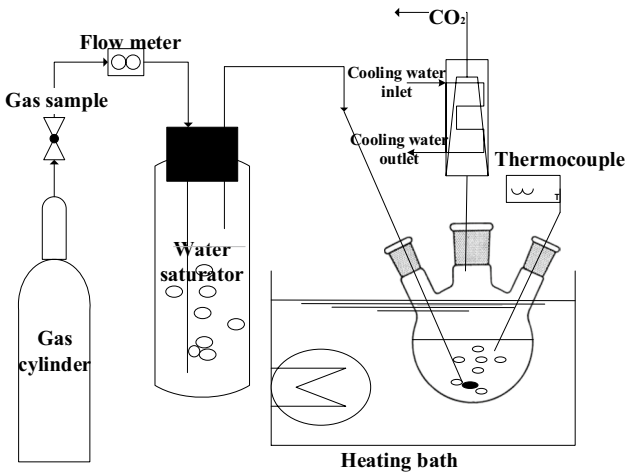

Fig. 1 Equipment setup

Methodology

Experiments

Materials and chemicals

Three solvents purchased from Sigma-Aldrich, CA, were monoethanolamine (MEA) (> 0.99 purity), 2-(butylamino) ethanol (BEA) (> 0.98 purity), and 2-amino-2-methyl-1-propanol (AMP) (> 0.90 purity); deionized water and 8, 15.1, 30, and 50 vol.% CO_2 (N_2 balanced) gas cylinders were supplied by Praxair Inc., Canada (analytical uncertainty ± 2% rel); 1 N hydrochloric acid (HCl) was purchased from Fisher Chemical, USA (> 0.995 purity).

Equipment setup and uncertainties

A schematic drawing of the CO_2 solubility apparatus is shown in Fig. 1. A three-neck round-bottom flask filled with 30 mL of solvent was placed inside the silicone oil heating bath (PolyScience PD Performance Digital 7 L Heat Bath; Cole-Parmer, Canada), which was specified to be 313 K and 363 K. The temperature of the solvent was measured using an electronic thermometer (Oakton Acorn Temp JKT series, ± 0.25%). Once the desired temperature was reached, the dry feed gas (8 to 50 vol.% CO_2 with N_2 balanced) was introduced to the water saturator

(100 mL) before the saturated gas was introduced to the flask to react with the solvent. The IR analyzer (Nova Analytical Systems Inc., USA) was used to manually calibrate the gases to ensure that the desired CO_2 partial pressure in the feed gas was applied, which relates to the uncertainty of the CO_2 partial pressure. The experiments of this work were done in low-pressure regions. Hence, the experimental data were collected under atmosphere pressure. To ensure that the feed gas fully interacted with the solvent, the proper gas flow rate (0.3 ± 0.02 SLPM) was manually controlled by the needle valve and monitored by the digital gas flow meter (EW-32908–73; Cole-Parmer, USA). The experiments required at least 6 h of the duration to achieve the equilibrium loading depending on the given temperature, pressure, and type of solvent. CO_2 loading was measured at least twice for each trial every 2 h and the average taken. After 6 h, CO_2 loading was measured at a time interval of a half hour. The equilibrium was achieved when the latest two consecutive measurements of CO_2 loading were observed to be extremely close to each other with a 3% maximum acceptable difference introduced by several previous studies that used the same experiment method (Narku-Tetteh et al. 2017a, b; Li et al. 2021). The CO_2 loading measurements were done by using the Chittick apparatus to titrate the specific volume of the solvent sample with a standard 1 N hydrochloric acid (HCl) and using 0.1 wt.% of methyl-orange solution as a color indicator. Besides, a condenser was installed to the gas outlet of the flask to avoid amine vaporization losses. The cooling water (7 °C) in the condenser was circulated through the circulating chiller (Isotemp, Fisher Scientific, Canada). The condensed amine was flowed back to the flask after condensation to maintain the identical volume of the amine solvent in the reactor. No sediment appeared in the solution at the end of the experiments.

The CO_2 loading could be determined through the ratio of moles of absorbed CO_2 and moles of amine solvent. In this work, the solvent sample ($1 \text{ mL} \pm 0.005$ mL) was taken to analyze the CO_2 loading, sealing everything properly for the HCl titration work. The volume of CO_2 was captured when CO_2 was released from the amine sample. Mole CO_2 and mole amine could then be calculated through Eqs. 1 and 2, respectively.

$$n_{CO_2} = \frac{V_{CO_2} \times \rho_{CO_2}}{MW_{CO_2}} \tag{1}$$

$$n_{amine} = V_{amine} \times C_{amine} \tag{2}$$

where V_{CO_2} represents the volume of CO_2 captured through the titration method; ρ_{CO_2} represents the density of CO_2; MW_{CO_2} represents the molecular weight of CO_2 (44 g/mol); V_{amine} represents the volume of the amine sample (1 mL); and C_{amine} represents the concentration of amine in moles per liter.

The evaluation of the heat of CO_2 absorption was also reported in this work. To accomplish this objective, the Gibbs–Helmholtz equation (Eq. 3) (Narku-Tetteh et al. 2017a, b) was applied to estimate the heat of absorption (ΔH_a). From Eq. 3, ΔH_a can be determined from the slope of the plot between $\text{Ln}(P_{CO_2})$ and $1/T$. Considering temperature and CO_2 partial pressure as two variables, the variation of CO_2 solubility in the identical solvent could be eventually affected. Thus, it is essential to find the CO_2 solubility at various temperatures (absorption condition). Several additional equilibrium CO_2 solubility experiments in bi-solvents at temperature (298 K) and CO_2 partial pressure (15.3 kPa) were conducted in this work.

$$\frac{\Delta H_a}{R} = \frac{d(\text{Ln}(P_{CO_2}))}{d(\frac{1}{T})} = \frac{[\text{Ln}(P_{CO_2})]_{313K} - [\text{Ln}(P_{CO_2})]_{298K}}{[1/T]_{298K} - [1/T]_{313K}} \tag{3}$$

where R is the universal gas constant (J/mol.K).

The uncertainties of this experiment consist of several possible system errors, including temperature ($u(T_1) = 0.8$ K (at 313 K); $u(T_2) = 0.9$ K (at 363 K)), the volume of the solvent in the reactor ($u(V_1) = 0.01$ mL), the volume of the sample solvent for the measurement of CO_2 loading ($u(V_2) = 0.005$ mL), and pressure $u(P) = 0.5$ kPa. The overall uncertainty for the measurement of CO_2 solubility can be calculated in the same way as introduced by He et al. (2021). All estimated uncertainties are listed behind the experimental results that will be discussed in the next chapter.

Artificial neural network preparation

ANN is a great computing tool, which could provide strong data processing ability. In this work, the experiments of CO_2 solubility were investigated in a wide temperature range from 313 to 363 K. ANN has excellent classification capacity and data learning abilities to process various solvent blends with different amine concentration ratios at a wide range of operating conditions. The feed-forward multilayer neural network is a typical form of ANN. It is normally composed by one input layer, one or more hidden layer(s), and one output layer. Figure 2 indicates that the selected input data are able to be processed based on the collection of connected neurons, and the signal of selected information is produced and transmitted to other neurons. Consequently, it can be computed to the final output layer through a nonlinear function. Through the computation process, data are transmitted in numbers, thus normalizing data is the fundamental step before training the model as shown in Eq. 4. In the

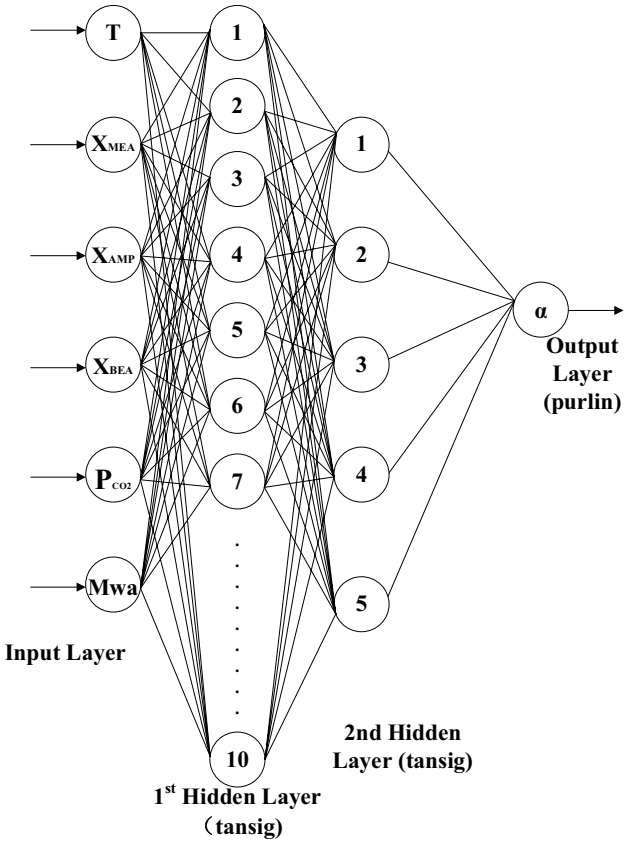

Fig. 2 Model structure

meantime, the numbers provide more appropriate strength for the connections of the neurons. For the exact purpose of extracting desired outputs, researchers are thus able to adjust the weight and bias based on a training algorithm (Kent and Eisenberg 1976). The weight of each connection between the neurons are estimated upon the importance of each neuron. In the past decade, researchers (Liu et al. 2019) found that backpropagation neural networks (BPNN) and radial basis function neural networks (RBFNN) are two promising learning algorithms to predict CO_2 solubility in the amine system. Liu et al. (2019) developed BPNN and RBFNN to predict the CO_2 in seven different single solvents. Their predictions were then compared with the predictions using six various thermodynamic models, including the Kent-Eisenberg model (Kent and Eisenberg 1976), Austgen model (Austgen et al. 1991), Li-Shen model (Li and Shen 1993), Hu-Chakma model (Hu and Chakma 1990), Liu-Helei model (Liu et al. 2019), and Liu's model (Liu et al. 2017a, b); the results demonstrated that BPNN exhibited the closest predictions to the experimental data compared to others when the solvent was completely dissolvable. BPNN could provide better predictions due to its advantage of error backpropagation (Sipocz et al. 2016). Therefore, users are allowed to re-train the network by adjusting the initial generated weights and biases (Fu et al. 2013; Li et al. 2021; Chen et al. 2015). Levenberg–Marquardt (LM) is a training algorithm commonly applied in the feed-forward multilayer neural network, which is specifically designed to minimize the sum-of-square error functions for nonlinear systems as a combination of gradient descent and Gauss–Newton methods (Li et al. 2021). Typically, there are two nonlinear activation functions applied to transform the information from layer to layer, named as Tan-sigmoid (tansig) and Log-sigmoid (logsig). Li et al. (2021) compared these two functions in two model structures. The results indicated that there is no significant difference between two transfer functions. However, the network with the tansig transfer function predicts slightly more accurate CO_2 loadings than the network with the logsig transfer function when they checked the mean square error. From previous studies (Chen et al. 2015; Hamzehie et al. 2014; Murshid et al. 2020; Golzar et al. 2016), it was found that the feed-forward multilayer neural network trained with the Levenberg–Marquardt back-propagation algorithm is beneficial to predict CO_2 solubility in the amine system. However, the number of the hidden layers and the neurons are varied by several conditions, such as training data, input data type, outputs, weight and bias, and others. Thus, it is essential to determine the most appropriate model structure for this study.

$$Y_i = \frac{(x_i - x_{\min})}{(x_{\max} - x_{\min})} \tag{4}$$

where Y_i is the normalized training and testing data sets; x_i is the training and testing data sets; and $x_{\min}$ and $x_{\max}$ are the minimum and the maximum values of variable, respectively.

In this work, the feed-forward multilayer neural network model was developed based on the Levenberg–Marquardt backpropagation algorithm by using the MATLAB toolbox. Five hundred data were obtained from several reliable published experimental works. Specifically, 85% of them were randomly applied to train the model, while 15% of data were randomly selected for validation. It should be noticed that all training data and testing data were collected from the open sources (see Table 1); while the experimental results of this work were only used as sample data, the training data will not be used as testing data repeatedly. The data was transmitted in the hidden layers through the tansig nonlinear transfer function, while the output layer was set as the Purlin linear function for fitting function problems for the sigmoid output neurons (Li et al. 2021). The investigations of CO_2 solubility were strongly affected by several parameters, including temperatures, CO_2 partial pressures, amine type, and amine concentration ratios. Therefore, the input data of the model were thus composed by the above four elements. Specifically, the apparent molecular weight was considered as an input parameter because it helps the system recognize the solvent type. This work investigated several bi-solvents and

Table 1 Data collection

References	Input						Target	
	T (K)	X_{MEA} (wt.%)	X_{AMP} (wt.%)	X_{BEA} (wt.%)	P_{CO_2}(kPa)	MWa (g/mol)	α (mol/mol)	Data points
Tontiwachwuthikul et al. (1991)	293–353	0	18–28	0	1.59–98.93	16.23–24.54	0.126–0.96	40[b, c]
Li and Chang (1995)	313–353	13–19	18–28	0	0.55–148.90	27.70–32.20	0.116–0.603	64[b]
Hwang et al. (2017)	313–393	0	0	15–30	0.04–348.24	16.94–35.98	0.077–0.992	46[b, c]
Narku-Tetteh et al. (2017a, b)	313–363	0–30	0–24	0–64	8–100	7.53–74.78	0.240–0.810	83[a, b, c]
Aronu et al. (2011)	313	15–45	0	0	0.0016–16	15–45	0.102–0.565	46[b, c]
Shen and Li (1992)	313	15–30	0	0	5–552	15–30	0.471–0.873	15[b, c]
Teng and Mather. (1990)	313–343	0	18	0	0.16–791	16	0.033–1.026	20[b, c]
Pahlavanzadeh et al. (2011)	293–323	0	9–37	0	17–70	8.10–33.00	0.044–0.947	57[b, c]
Choi et al. (2020)	323–383	9–21	9–22	0	0.03–333.50	20.93–24.90	0.028–0.782	68[b, c]
Kundu et al. (2003)	303–323	0	18–31	0	3.25–91.50	16.26–27.89	0.412–0.966	51[b, c]
Singh et al. (2011)	313	3–15	0	0	0.88–39.48	1.88–9.40	0.490–0.760	10[b, c]

[a]Modified data from the given figures and the exponential equation

[b]Applied in ANN modeling

[c]Applied in KE modeling

tri-solvents; all solvents were composed of MEA with AMP or/and BEA. To improve the learning ability of the model, the amine concentration should be divided as the weight fraction of MEA, AMP, and BEA as shown in Fig. 2, and can be defined as Eq. 5 below. The number of neurons and hidden layers was affirmed by comparing the mean square errors (MSE) and the correlation coefficient (R^2) of their predictions as shown in Eqs. 6 and 7 (Li et al. 2021).

$$\alpha_{CO_2} = f(X_{MEA}, X_{AMP}, X_{BEA}, MWa, P_{CO_2}, T) \tag{5}$$

$$MSE = \frac{1}{N}\sum_{i=1}^{N}\left(\alpha^{exp} - \alpha^{predicts}\right) \tag{6}$$

$$R^2 = 1 - \frac{\sum_{i=1}^{N}(\alpha^{predicts} - \alpha^{exp})^2}{\sum_{i=1}^{N}(\alpha^{exp} - \overline{\alpha}^{exp})^2} \tag{7}$$

where N represents the total number of data points; α^{exp} represents the experimental result of CO_2 loading; $\alpha^{predicts}$ represents the prediction results of CO_2 loading; and $\overline{\alpha}^{exp}$ represents the mean of the experimental CO_2 loading.

Table 1 lists the available data sources of CO_2 solubility in MEA, AMP, and BEA and their blends. The data set covers a temperature range between 293 and 393 K, a CO_2 pressure range between 0.0016 and 791 kPa, and a total amine concentration up to 6 mol/L (Tontiwachwuthikul et al. 1991; Li and Chang 1995; Hwang et al. 2017; Narku-Tetteh et al. 2017a, b; Aronu et al. 2011; Shen and Li 1992; Teng and Mather 1990; Pahlavanzadeh et al. 2011; Choi et al. 2020; Kundu et al. 2003; Singh et al. 2011). The rule of data collection of this work is that the input data must have a strong influence on the output quality. In this research, the majority of obtained experimental data are the CO_2 solubility at low pressures, because the input data should be relevant to the experimental data of this work. In general, it is difficult to identify an exact accurate amount of required data to train the model. These data mostly depend on the input and output parameters, as well as their relationships and complexity. The complexity is normally determined empirically, while the performance of the model can be evaluated by the error analysis. The screening of data is the key step of data selection before training the model; the lack of data or excess data are two undesired issues. Typically, the lack of input data could result in overfitting because the model cannot perform a well-learned behavior from insufficient given information, whereas too much irrelevant input data could increase the complexity of the model. Underfitting normally happens when the capacity of the model is too small, while excess capacity can also cause overfitting. To avoid such undesired issues, there is no conflicted input data collected in the dataset in order to reduce the complexity but maintain an excellent coverage. In addition, the proper amount of data can also improve the stability of the final output. Thus, ANN can learn the training data strongly. The system can then automatically ignore the minority errors caused by the training data, which secure the prediction ability of the model. Murshid et al. (2020) studied that insufficient neurons could potentially cause the underfitted predictions compared to the experimental results, and an optimum number of neurons should be between 1 and 20 for a hidden layer. In conjunction with other published studies (Chen et al. 2015; Hamzehie et al. 2014; Murshid et al. 2020; Golzar et al. 2016), a comparison of various model structures with different neurons (1 hidden layer to 3 hidden layers) are summarized in Table 2. It can be observed from MATLAB

Table 2 Model structure

Hidden layer (MSE) #1_#2_#3	$R_{training}$	$R_{validation}$
10_0_0 (0.0058099)	0.89940	0.91240
15_0_0 (0.0056234)	0.92881	0.91998
20_0_0 (0.0051348)	0.92764	0.94881
8_4_0 (0.0041112)	0.93467	0.95361
8_5_0 (0.0042139)	0.95898	0.95112
9_4_0 (0.0058173)	0.96076	0.91283
9_5_0 (0.0038124)	0.96084	0.96276
10_5_0 (0.0032752)	0.96232	0.97388
10_7_0 (0.0051979)	0.93080	0.93202
15_5_0 (0.0051773)	0.91997	0.93428
15_7_0 (0.0052133)	0.95491	0.93189
20_7_0 (0.0049783)	0.92780	0.93987
20_10_0 (0.0045127)	0.93267	0.94275
10_5_2 (0.0049801)	0.91350	0.93912
10_6_3 (0.0033098)	0.92401	0.96611
10_7_1 (0.0044767)	0.90496	0.94512
15_10_5 (0.0045091)	0.95121	0.94120
20_10_5 (0.004677)	0.94328	0.94728

that two hidden layers with 10 (first layer) and 5 (second layer) neurons provided the best performance of prediction by comparing the correlation coefficient, which corresponds to the lowest MSE (0.0032752) compared to other structures. The lower the MSE, the more accurate the prediction. Therefore, the structure (see Fig. 2) was applied for the further predications of this study based on the specific input parameters and training algorithm. The edited weights and biases were continuously updated to achieve the desired prediction. However, the structure of the model could also decide the learning ability of the model. Hence, the error was recorded once it was no longer changed significantly. The next structure was tested and compared with the others. Table 3 shows the weights of the connections between the input variable and its corresponding neuron on the first hidden layer, while Table 4 shows the weights of the connections between the neuron on the first hidden layer to its corresponding neuron on the second hidden layer and the biases of the neuron on the second hidden layer to the output layer.

Once the model was ready, it was utilized to correlate the sample data, which were all selected from the experimental results of this research. In order to ensure that the deviation was not caused by the experiment, the experiment required to be repeated if the corresponding deviation was too large ($> 10\%$). The deviation would be finally recorded if the repeated experimental result was consistent to the previous experimental result. This step increases the reliability of the experimental results. The equation of deviation estimation is introduced in the next section.

Kent-Eisenberg modeling

The KE model is employed to correlate the CO_2 solubility in several amine blends, including MEA/AMP, MEA/BEA, and MEA/AMP/BEA. The objective of this work is going to build a simplified KE model which is fitted for both bi-solvents and tri-solvents on the basis of only single-amine VLE data. To accomplish this target, the procedures can be summarized into six major steps:

(i) A nonlinear equation was initially developed to describe the chemical and physical equilibria in CO_2-amine systems, and the electroneutrality balance formula was expressed to introduce all the ionic species.

(ii) The concentrations of all the ionic species were estimated by solving the nonlinear equation. The set of reaction in the CO_2-amine-water system is expressed below from Eq. 8 to Eq. 12 (Shi et al. 2021a, b; Hwang et al. 2017).

Dissociation of bicarbonate ion:

$$HCO_3^- \overset{K1}{\Longleftrightarrow} CO_3^{2-} + H^+ \tag{8}$$

Formation of bicarbonate:

Table 3 Weights and biases for the first two layers

Number of the neuron on the 1st hidden layer	Weights						
	X_{MEA}	X_{AMP}	X_{BEA}	P_{CO_2}	Mwa	T	*Biases*
1	1.003	0.397	−0.377	−4.689	0.363	−1.693	−2.361
2	1.630	1.342	2.509	1.401	−2.734	−1.152	4.923
3	−0.732	−1.106	−2.724	−9.921	2.131	5.575	−9.877
4	0.019	−0.734	−2.346	6.731	2.467	3.379	6.714
5	1.062	1.445	3.461	−2.345	−3.030	−8.422	−2.760
6	6.975	2.263	4.573	−0.830	2.388	3.379	13.705
7	−0.673	−11.641	−1.278	−2.729	−3.850	3.688	6.061
8	3.782	−3.762	7.729	−1.242	−1.612	−5.356	0.389
9	−11.538	−2.008	1.380	13.924	−2.227	−4.030	−0.152
10	2.439	−0.929	−1.836	−0.134	5.660	3.957	6.077

Table 4 Weights and biases for the other layers

Number of the neuron on the 2nd hidden layer	Weights										Weights	
	Number of the neuron on the 1st hidden layer										Output layer	
	1	2	3	4	5	6	7	8	9	*10*	*Biases*	α	*Biases*
1	−0.793	−1.326	−0.252	0.152	−0.378	3.217	0.388	0.395	0.334	−4.082	4.509	4.123	−5.565
2	−0.166	−0.768	0.102	−0.153	−0.189	5.634	5.176	0.211	−0.236	−3.692	−7.520	−3.472	
3	−6.064	5.185	−20.264	3.957	−14.373	−1.810	2.344	0.665	−2.174	2.287	0.992	10.13	
4	−2.899	−3.806	1.761	−6.414	−2.679	4.168	−4.458	−3.679	4.664	−8.051	−3.950	9.751	
5	0.843	1.386	−1.001	−2.774	0.249	3.789	0.551	−1.238	0.514	−2.901	2.380	−1.599	

$$CO_2 + H_2O \overset{K2}{\Longleftrightarrow} HCO_3^- + H^+ \tag{9}$$

Dissociation of water:

$$H_2O \overset{K3}{\Longleftrightarrow} OH^- + H^+ \tag{10}$$

Deprotonation of amines:

$$AmineH^+ \overset{K4}{\Longleftrightarrow} Amine + H^+ \tag{11}$$

Carbamate hydrolysis:

$$AmineCOO^- + H_2O \overset{K5}{\Longleftrightarrow} Amine + HCO_3^- \tag{12}$$

where amine represents MEA or AMP or BEA. It should be noted that AMP carbamate is considered in this work. The previous research indicated that AMP carbamate should be considered although the concentration of AMP carbamate is low (Xu et al. 1992). From previous work (Shi et al. 2021a, b), AMP carbamate is considered when using 2 mol/L AMP-based blended solvents. In this case, the KE model of this work should consider AMP carbamate.

The equilibrium constants can thus be expressed as below:

$$K_1 = \frac{[CO_3^{2-}][H^+]}{[HCO_3^-]} K_2 = \frac{[HCO_3^-][H^+]}{[CO_2]}, K_3 = [H^+][OH^-]$$

$$K_4 = \frac{[Amine][H^+]}{[AmineH^+]}, K_5 = \frac{[Amine][HCO_3^-]}{[AmineCOO^-]}$$

where K_i is the equilibrium constant. The estimated concentration of CO_2 in the liquid phase can be calculated from Henry's law as shown in Eqs. 13 and 14 (Hwang et al. 2017):

Physical solubility

$$CO_2(g) \overset{H_{CO_2}}{\Longleftrightarrow} CO_2(aq) \tag{13}$$

$$P_{CO_2} = H_{CO_2}[CO_2] \tag{14}$$

(iii) MATLAB was applied to determine the unknown equilibrium constants. Equilibrium constants and Henry's constant (Hwang et al. 2017; Kent and Eisenberg 1976; Edwards et al. 1978; Hamborg and Versteeg 2009; Silkenbaumer et al. 1998; Rumpf and Maurer 1993) were determined by using Eq. 15 (Edwards et al. 1978) with the parameters summarized in Table 5.

$$K_i \text{or} H_{CO_2} = \text{EXP}\left(\frac{a_i}{T} + b_i \ln T + c_i T + d_i\right) \tag{15}$$

In the liquid system, the balance of amine, CO_2, and charge is expressed as the following equations (Eq. 16 to Eq. 18):

Table 5 Equilibrium constants and Henry's constants

Parameter[a]	a_i	b_i	c_i	d_i	Range of validity (K)	Reference
K_1	−12,431.7	−35.482	0	220.067	273–498	Edwards et al. (1978)
K_2	−12,092.1	−36.782	0	235.480	273–499	Edwards et al. (1978)
K_3	−13,445.9	−22.477	0	140.932	273–500	Edwards et al. (1978)
$K_{4,\,MEA}$	−17.3	0.058	0	−38.846	293–353	Hamborg and Versteeg (2009)
$K_{5,\,MEA}$	−3090.8	0	0	6.694	293–413	Kent and Eisenberg. (1976)
$K_{4,\,AMP}$	−16.7	0	0.621	−41.000	298–353	Hamborg and Versteeg. (2009)
$K_{5,\,AMP}$	2546.2	0	0	−11.555	298–314	Silkenbaumer et al. (1998)
$K_{4,\,BEA}$	−5997.0	0	0	−3.460	313–393	Hwang et al. (2017)
$K_{5,\,BEA}$	3997.0	0	0	−12.460	313–394	Hwang et al. (2017)
H_{CO_2}	−9624.4	−28.749	0.014	192.876	273–473	Rumpf and Maurer. (1993)

[a]In molarity basis

Amine balance:

$$[\text{Amine}]_t = [\text{Amine}] + \left[\text{AmineH}^+\right] + [\text{AmineCOO}^-] \quad (16)$$

CO_2 balance:

$$\alpha_{CO_2} \times [\text{Amine}]_t = \left[CO_2\right] + \left[HCO_3^-\right] + \left[CO_3^{2-}\right] + [\text{AmineCOO}^-] \quad (17)$$

Electroneutrality balance (charge balance):

$$\left[H^+\right] + \left[\text{AmineH}^+\right] = \left[HCO_3^-\right] + 2\left[CO_3^{2-}\right] + [OH^-] + [\text{AmineCOO}^-] \quad (18)$$

After the derivation, a single polynomial equation is shown in Eq. 19, which is a combination of the hydrogen ion concentration and the equilibrium constants.

$$A[H^+]^5 + B[H^+]^4 + C[H^+]^3 + D[H^+]^2 + E\left[H^+\right] + F = 0 \quad (19)$$

where

$$A = K_5$$

$$B = K_4K_5 + [\text{Amine}]_tK_5$$

$$C = K_2K_4\frac{P_{CO2}}{H_{CO2}} - K_2K_5\frac{P_{CO2}}{H_{CO2}} - K_3K_5$$

$$D = -K_2K_4K_5\frac{P_{CO2}}{H_{CO2}} - 2K_1K_2K_5\frac{P_{CO2}}{H_{CO2}} - K_3K_4K_5 - K_2K_4\frac{P_{CO2}}{H_{CO2}}[Amine]_t$$

$$E = -K_2^2K_4\frac{P_{CO2}}{H_{CO2}}^2 - 2K_1K_2K_4K_5\frac{P_{CO2}}{H_{CO2}} - K_2K_3K_4\frac{P_{CO2}}{H_{CO2}}$$

$$F = -2K_1K_2^2K_4\frac{P_{CO2}}{H_{CO2}}^2$$

The initial CO_2 loadings were eventually determined by using the simplified equation (Eq. 20).

$$\alpha = \frac{\frac{P_{CO2}}{H_{CO_2}}\left[1 + \frac{K_2}{[H^+]} + \frac{K_1K_2}{[H^+]^2} + \frac{K_2K_4[\text{Amine}]_t}{K_4K_5[H^+] + K_5[H^+]^2 + K_2K_4\,{}^{P_{CO2}}/_{H_{CO_2}}}\right]}{[\text{Amine}]_t} \quad (20)$$

(iv) The developed models were validated with available experimental data from several publications.

(v) K_4 and K_5 were regressed to fit the experimental data with the model expression, which was previously discussed by Mondal et al. (2017). As they mentioned before, the generalized reduced gradient nonlinear optimization technique is suggested to use to improve the prediction accuracy, hence the objective function (Eq. 21) must be inserted to MATLAB in order to have the error analysis.

$$\%\text{AAD} = \frac{1}{N}\sum_{i=1}^{N}\left|\frac{\alpha_{CO_2,i}^{Ex} - \alpha_{CO_2,i}^{Cal}}{\alpha_{CO_2,i}^{Ex}}\right| \quad (21)$$

where $\alpha_{CO_2,i}^{Ex}$ and $\alpha_{CO_2,i}^{Cal}$ are the experimental and predicted CO_2 loadings, respectively; N represents the total number of data (Mondal et al. 2017).

It was studied by Haji-Sulaiman et al. (1998) that K_i is originally a single function which is only related to temperature. Thus, an additional factor F_i should be considered as the effects in terms of CO_2 partial pressure and the amine concentration. Consequently, the modified K_i can be expressed as K_i', as shown in Eq. 22 (Haji-Sulaiman et al. 1998):

$$K_i' = K_iF_i \quad (22)$$

A simplified form of F_i was also introduced by Haji-Sulaiman et al. (1998) as the following equations:

Protonation of amine:

$$F_i = g_i \mathrm{LnP}_{\mathrm{CO}_2} + k_i \mathrm{Ln}[\mathrm{amine}] \quad (23)$$

Formation of carbamate:

$$F_i = g_i \mathrm{LnP}_{\mathrm{CO}_2} + j_i / [\mathrm{amine}] \quad (24)$$

The regression was completed by using the MATLAB optimization toolbox. The constrained optimization function "*fminunc*" command was applied in this present work. It should be noted that the step of regression is always established upon sufficient vapor–liquid equilibrium (VLE) data. The data set should cover the CO_2 solubility in different concentrations of amine solvent at wide ranges of temperature and pressure. In general, substantial VLE data of the single solvents are available on different publications. However, the study of blended solvents is very insufficient, particularly for the tri-solvents. The lack of available experimental VLE data of the MEA/BEA and MEA/AMP/BEA blends are the major knowledge gap for regressing the model and validating the model.

(vi) Considering these limitations, the authors decided to build a simplified KE model on the basis of single amine. The MEA model was regressed based on 89 data from Narku-Tetteh et al. (2017a, b) and Aronu et al. (2011). The AMP model was regressed based on 113 data from Teng and Mather (1990), Pahlavanzadeh et al. (2011), and Kundu et al. (2003). The BEA model was regressed based on 47 data from Narku-Tetteh et al. (2017a, b) (for details, see Table 1). Consequently, the estimated CO_2 solubility in blended solvent can be calculated by mole fraction weighting of each single amine from the following Eq. 25 (Shi et al. 2021a, b).

$$\alpha_{\mathrm{Cal,blends}} = \frac{C_{\mathrm{MEA}} \bullet \alpha_{t,\mathrm{MEA}}^{\mathrm{Cal}} + C_{\mathrm{AMP}} \bullet \alpha_{t,\mathrm{AMP}}^{\mathrm{Cal}} + C_{\mathrm{BEA}} \bullet \alpha_{t,\mathrm{BEA}}^{\mathrm{Cal}}}{C_{\mathrm{total}}} \quad (25)$$

where $\alpha_{\mathrm{Cal,blends}}$ is the estimated equilibrium loading for amine blends; C_{MEA}, C_{AMP}, and C_{BEA} are the concentrations of MEA, AMP and BEA, respectively; and $\alpha_{t,\mathrm{MEA}}^{\mathrm{Cal}}$, $\alpha_{t,\mathrm{AMP}}^{\mathrm{Cal}}$, and $\alpha_{t,\mathrm{BEA}}^{\mathrm{Cal}}$ are the estimated loadings generated by each single-amine model when the total amine concentration was input.

Results and discussions

Experiment validation

The experiment was validated by measuring the CO_2 solubility in 2.5 mol/L aqueous MEA solvent at 313 K. The percentage of average absolute deviation (%AAD) (Eq. (21)) represents the deviation between the experimental results of this work and the published data from several sources presented in Table 6. Furthermore, it is essential to find the relationship between the CO_2 partial pressure and CO_2 loading for the experimental data of this work, since the published data were completed at different pressures. Thus, the estimated CO_2 loading (this work) was calculated from the exponential equation as shown in Fig. 3, which could cover all CO_2 loadings under varied specific CO_2 partial pressures obtained from the published data. Table 6 confirms that the measured data were in good agreement with the published data (Shen and Li 1992; Portugal et al. 2009; Mazinani et al. 2011), particularly compared to the data reported by Shen and Li. (1992) and Mazinani et al. (2011). A relatively higher %AAD was observed when the measured data was compared to Portugal's data (2009). It could be explained by several reasons: (i) slight difference from the MEA mass fraction; (ii) varied purity of the chemical; (iii) since an exponential equation was developed at a CO_2 pressure range between 8 and 50 kPa, a higher deviation thus appeared when predicting the CO_2 loading under 8 kPa.

For the work of KE modeling, Table 7 shows the final regressed parameters applied in this modeling section. As mentioned in "Methodology," the predictions of CO_2 solubility were computed based on the predictions of three single-amine KE models. In order to validate the prediction reliability of the corresponding model, this work used several testing data to justify three single-amine models. All testing data are summarized in Table 1. The MEA model was validated by using the 22 available data reported by Shen et al. (1992) and Singh et al. (2011) as shown in Fig. 4(a). The model finally contributed 4.68% of %AAD. The AMP model was validated by 32 available data provided by Tontiwachwuthikul et al. (1991) as shown in Fig. 4(b), and AAD% was calculated as 8.43%. The BEA model was validated by 33 available data provided by Hwang et al. (2017) as shown in Fig. 4(c), and %AAD was found as 14.64%.

Table 8 indicates the comparison between the estimated CO_2 loading by using the proposed modeling approach and 23 experimental data (Choi et al. 2020) at specific temperature and pressure. It exhibited 20.39% of %AAD, and the most obvious deviation was observed when the CO_2 partial pressure is below 5 kPa or greater than 250 kPa. However, the objective of the experiments of this study was completed at a CO_2 partial pressure range between 8 and 50 kPa. If %AAD only counted the CO_2 loading at the pressure ranges from 5 to 250 kPa, it would decrease to 9.06%. Compared to other published studies (Kent and Eisenberg 1976; Haji-Sulaiman et al. 1998), the predictions of this work exhibited an acceptable deviation. Therefore, this approach is an applicable method to correlate the experimental results of this research.

CO_2 solubility in the aqueous MEA/AMP blends

The experimental results of CO_2 solubility in aqueous MEA-AMP blends are summarized in Table 6. This work

Table 6 Experiment validation at the CO_2 partial pressure range between 1.02 and 120.7 kPa

Experimental data			Estimated loading	Deviation	%AAD
P_{CO_2}(kPa)	CO_2 loading (uncertainty)	Sources	$P_{CO_2}= 0.0024e^{15.703\alpha}$		
8.104	0.519 (0.0014)	This work	0.517		
15.30	0.552 (0.0009)		0.557		
30.39	0.602 (0.0005)		0.602		
50.65	0.633 (0.0004)		0.634		
1.02	0.471	Portugal et al. (2009)	0.385	18.172*	8.748
2.11	0.491		0.432	12.078	
21.1	0.621		0.578	6.871	
41.4	0.635		0.621	2.165	
62.8	0.678		0.648	4.456	
4	0.505	Mazinani et al. (2011)	0.472	6.449	2.678
14	0.537		0.552	2.832	
20	0.570		0.575	0.864	
26	0.595		0.592	0.566	
15.7	0.561	Shen and Li. (1992)	0.560	0.266	2.001
24.1	0.609		0.588	3.646	
35.3	0.619		0.611	1.276	
55.6	0.641		0.640	0.150	
89.4	0.685		0.670	2.149	
120.7	0.722		0.689	4.516	

*Calculation example: (0.471–0.385)/0.471

maintained the concentration of AMP at 2 mol/L, while the concentration of MEA was varied at 0.1, 0.3, and 0.5 mol/L, respectively. It is known that the CO_2 solubility normally decreased by increasing the operating temperature, while it increased by increasing the operating pressure (Tontiwachwuthikul et al. 1991).

Adding an additional small volume of MEA (from 0.1 to 0.5 mol/L) into the aqueous AMP solvent can eventually cause two distinct influences on the CO_2 solubility as shown in Table 9. At 313 K, increasing MEA concentration could decrease the CO_2 loading significantly. The temperature of 363 K, which could often be used in the desorption process, was considered as the desorption condition. Typically, CO_2 solubility in the aqueous MEA solvent is higher than that in the aqueous AMP solvent at high temperature. Researchers thus suggested that AMP solutions are superior to MEA solutions for the regeneration process of CO_2 (Tontiwachwuthikul et al. 1991). Therefore, the higher concentration of MEA in the aqueous AMP solvent could conceptually increase the CO_2 solubility at high temperature. At both two conditions, the phenomena when adding addition MEA into the aqueous AMP solvent are unfavorable for CO_2 capture. However, a comprehensive study should also cover the acceleration of the CO_2 absorption rate and the regeneration energy demand. Kinetics does not

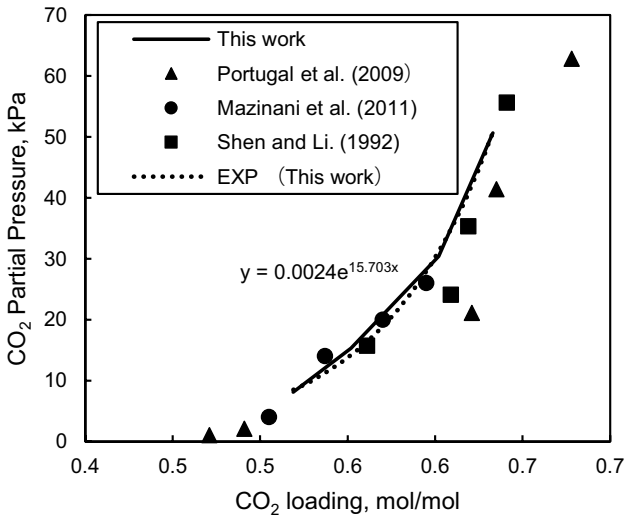

Fig. 3 Experiment validation at the CO_2 partial pressure range between 1.02 and 120.7 kPa

Table 7 Computed regression parameters for the single solvent KE models

	g_i	k_i	j_i
$F_{1,MEA}$	0.4842	0.508	0
$F_{2,MEA}$	−0.12002	0	0.8204
$F_{1,AMP}$	−0.05842	0.187	0
$F_{2,AMP}$	−0.002166	0	−0.000334
$F_{1,BEA}$	0.0902	0.856	0
$F_{2,BEA}$	0.1566	0	0.8211

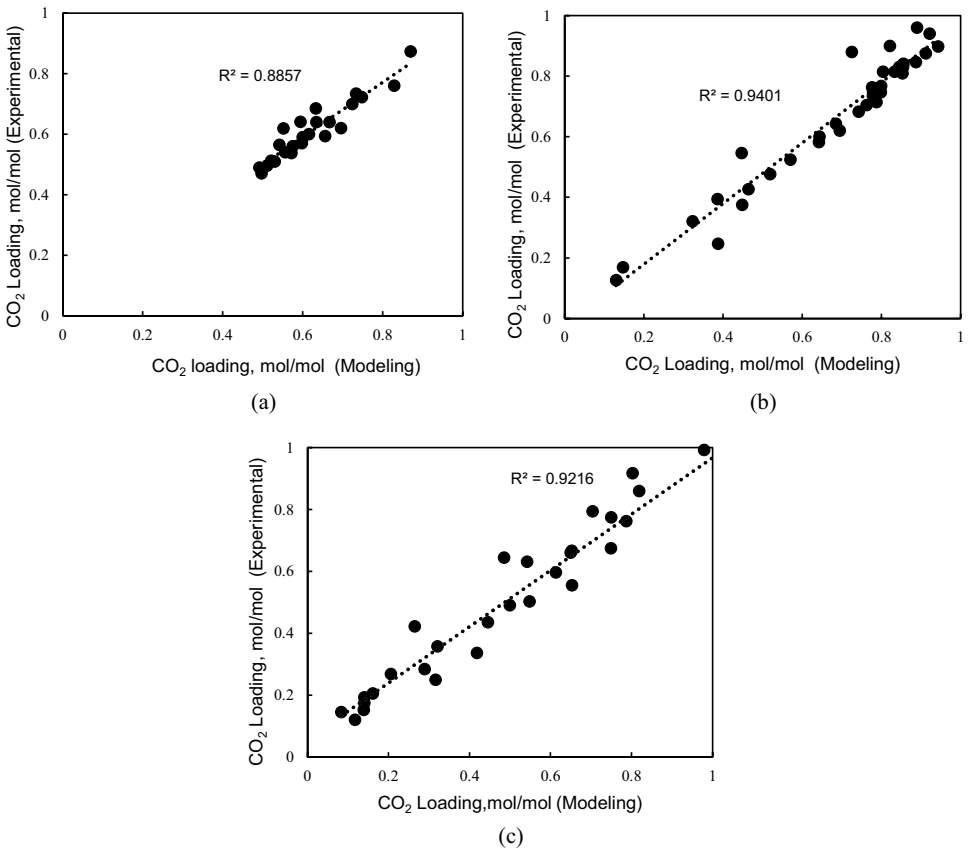

Fig. 4 Validation of three single solvent KE models. **a** MEA. **b** AMP. **c** BEA

affect the equilibrium solubility of CO_2, but it simply reflects how fast a solvent can achieve to equilibrium at specific temperature and pressure. From a previous published achievement (Shi et al. 2021a, b), the analysis of the coordinative effect of MEA + AMP solvents was comprehensively studied on both absorption and desorption. Despite that the CO_2 absorption capacity of MEA is lower than that of AMP, it still provides a stronger absorption rate than AMP, which could be considered as an additional benefit for CO_2 capture (Shi et al. 2021a, b). It was also mentioned by Shi et al. (2021a, b) that the coordinative effect of addition MEA (0.1–0.5 mol/L) into AMP is negligibly small due to the weak carbamate stability of AMP. By comparing with 2 mol/L AMP, adding addition MEA (0.1–0.5 mol/L) can enhance up to 8% of the absorption rate, but the enhancement did not exhibit regulated changes by increasing the volume of addition MEA (Shi et al. 2021a, b).

It is also observed that the volume of added MEA is a considerable influencing factor on the solubility of CO_2. A more significant impact was observed when the concentration of MEA was increased from 0.1 to 0.3 mol/L compared to the increase in MEA concentration from 0.3 to 0.5 mol/L. Considering the solubility of CO_2 alone, MEA + AMP blends are significantly higher than MEA single solvent. Taking 15 kPa as an example, replacing 2.5 mol/L MEA by MEA + AMP (0.5 + 2 mol/L) leads to an enhancement in the CO_2 solubility by about 19%, which could be observed by comparing the data in Table 9 with the data given in Fig. 3.

CO_2 solubility in the aqueous MEA/BEA blends

The present work investigated the CO_2 solubility in several aqueous MEA/BEA blends. Similar to the MEA concentration distributed in "CO_2 solubility in the aqueous MEA/AMP blends," the MEA concentration was varied at 0.1, 0.3, and 0.5 mol/L, then added into an identical amount of BEA (2 mol/L). A similar trend can be observed in Table 10 showing that the CO_2 solubility tends to decrease as the concentration of MEA was increased at 313 K, while the CO_2 solubility tends to slightly increase as the concentration of MEA was increased at 363 K. Compared to aqueous MEA/AMP blends, the effect of MEA on the CO_2 solubility in aqueous MEA/BEA at 313 K and 363 K was not significant. Promisingly, it is expected that an addition of MEA can significantly enhance the absorption rate and exhibit insignificant or mild impact on a reduction of absorption capacity. Interestingly, the absorption capacity of blended MEA-BEA fits well with this criterion by combining the present work with the previous study from Shi et al. (2021a, b).

Table 8 Prediction validation for blended solvents using the KE model

Mass fraction[a]		Total molar concentration (mol/L)	P_{CO_2}(kPa[a])	$\alpha_{MEA, cal}$	$\alpha_{AMP, cal}$	$\alpha_{blends, cal}$	$\alpha_{blends, exp}$[a]
MEA (wt.%)	AMP (wt.%)						
9	22	3.5	1.053	0.1076	0.1021	0.1037	0.122
9	22	3.5	2.520	0.2812	0.1554	0.1913	0.267
9	22	3.5	5.674	0.3186	0.3499	0.3410	0.403
9	22	3.5	18.998	0.4867	0.5980	0.5662	0.544
9	22	3.5	78.58	0.5273	0.6387	0.6069	0.655
9	22	3.5	165.705	0.5519	0.7577	0.6989	0.707
9	22	3.5	249.113	0.5974	1.0058	0.8891	0.738
9	22	3.5	333.458	0.7607	1.3896	1.2010	0.782
15	15	3.6	1.462	0.1209	0.0976	0.1312	0.125
15	15	3.6	2.899	0.3087	0.1719	0.2471	0.265
15	15	3.6	5.773	0.3125	0.3423	0.3259	0.404
15	15	3.6	23.87	0.4955	0.6231	0.5530	0.553
15	15	3.6	112.879	0.5589	0.6700	0.6090	0.654
15	15	3.6	221.563	0.5877	0.8488	0.7053	0.707
15	15	3.6	330.253	0.7261	1.3633	1.0131	0.742
21	9	4.5	1.515	0.1139	0.0982	0.1260	0.144
21	9	4.5	2.469	0.2145	0.3354	0.2414	0.28
21	9	4.5	7.091	0.3211	0.4111	0.3402	0.425
21	9	4.5	35.648	0.3528	0.5077	0.3872	0.553
21	9	4.5	130.261	0.5093	0.8563	0.5864	0.643
21	9	4.5	204.046	0.5313	0.9189	0.6174	0.675
21	9	4.5	277.018	0.5581	0.9383	0.6417	0.697
21	9	4.5	332.567	0.5924	1.1573	0.7193	0.717

[a]Data collected from Choi et al. (2020), CO_2 solubility at 323 K

CO_2 solubility in aqueous MEA/AMP/BEA blends

The CO_2 solubility data of the aqueous tri-solvent of MEA/AMP/BEA is shown in Table 11. The total concentration of AMP/BEA was maintained at 2 mol/L and 4 mol/L, respectively. For each of the solvent sample, the MEA concentration was varied at 0.1 mol/L, 0.3 mol/L, and 0.5 mol/L, while the molar ratio of AMP and BEA was 1:1. It can be observed that the increase in MEA concentration in the blended solvent could have less impact when the total AMP/BEA concentration was increased from 2 to 4 mol/L at both temperatures. This can be reasoned by the concentration of MEA which is accounted as a higher portion in 2 mol/L AMP/BEA blends. Since a fraction of MEA in 4 mol/L AMP/BEA decreased, its impact on CO_2 solubility then decreased. For the amine blends with identical volumes of MEA, the effect of CO_2 solubility strongly depended on the total amine concentration, temperature, and pressure. It was mentioned earlier that AMP is a typical sterically hindered amine, which is able to form unstable carbamate when reacting with CO_2. The unstable carbamate eventually hydrolyzed into bicarbonate; thus, the solvent blends with AMP exhibiting larger capacity allows more free amines to be available for the reaction with CO_2 (Coker et al. 2017). Taking MEA/BEA/AMP (0.1 ~ 0.5 + 1 + 1 mol/L) solvents as an example, the solubility of CO_2 is obviously higher than that in MEA/BEA (0.1 ~ 0.5 + 2 mol/L) at the same conditions as the data proposed in Table 10 and Table 11. This behavior contributed from the unstable carbamate of AMP. Similar to the observations from the two previous sections, the addition of MEA resulted in a decrease in CO_2 solubility, but the best recipe of the blended solvent should also consider the performance in mass transfer, absorption rate, and heat duty. According to a previous study (Shi et al. 2021a, b), MEA/BEA/AMP (0.3 + 2 + 2 mol/L) is recommended as the optimized ratio, which exhibited the strongest coordinative effect at both absorption and desorption conditions. Considering the CO_2 solubility data (Table 11) for MEA/BEA/AMP (0.1 ~ 0.5 + 2 + 2 mol/L) alone, a relatively regulated trend of reduction on CO_2 solubility could be observed by increasing the MEA concentration at 313 K, while there is no significant increase in CO_2 solubility when increasing the MEA concentration from 0.1 to 0.3 mol/L at 363 K, which is favorable for the desorption process.

Table 9 CO_2 solubility data in aqueous MEA/AMP blends

313.15 K[a]			363.15 Kb		
P_{CO_2}(kPa)	α (mol/mol)	$u(\alpha)$	P_{CO_2}(kPa)	α (mol/mol)	$u(\alpha)$
0.1 mol/L MEA + 2 mol/L AMP					
8.104	0.655	0.0022	15.296	0.297	0.0005
15.296	0.691	0.0013	30.390	0.372	0.0003
30.390	0.775	0.0007	50.650	0.411	0.0002
50.650	0.849	0.0005			
0.3 mol/L MEA + 2 mol/L AMP					
8.104	0.628	0.0019	15.296	0.295	0.0004
15.296	0.651	0.0011	30.390	0.363	0.0003
30.390	0.729	0.0007	50.650	0.401	0.0002
50.650	0.827	0.0005			
0.5 mol/L MEA + 2 mol/L AMP					
8.104	0.597	0.0019	15.296	0.304	0.0005
15.296	0.613	0.0011	30.390	0.355	0.0003
30.390	0.706	0.0007	50.650	0.391	0.0002
50.650	0.813	0.0005			

[a]Standard uncertainties are $u(T_1)=0.8$ K, $u(V_1)=0.01$ mL, $u(V_2)=0.005$ mL, $u(P)=0.5$ kPa at 313 K

[b]Standard uncertainties are $u(T_1)=0.9$ K, $u(V_1)=0.01$ mL, $u(V_2)=0.005$ mL, $u(P)=0.5$ kPa at 363 K, $u(V_1)=0.01$ mL, $u(V_2)=0.005$ mL, $u(P)=0.5$ kPa at 363 K

Table 10 CO_2 solubility data in aqueous MEA/BEA blends

313.15 K[a]			363.15 Kb		
P_{CO_2}(kPa)	α (mol/mol)	$u(\alpha)$	P_{CO_2}(kPa)	α (mol/mol)	$u(\alpha)$
0.1 mol/L MEA + 2 mol/L BEA					
8.104	0.597	0.0018	15.296	0.251	0.0004
15.296	0.624	0.0011	30.39	0.289	0.0002
30.390	0.688	0.0008	50.65	0.319	0.0002
50.650	0.722	0.0006			
0.3 mol/L MEA + 2 mol/L BEA					
8.104	0.588	0.0017	15.296	0.255	0.0004
15.296	0.606	0.0010	30.39	0.298	0.0002
30.390	0.669	0.0006	50.65	0.325	0.0002
50.650	0.706	0.0004			
0.5 mol/L MEA + 2 mol/L BEA					
8.104	0.577	0.0017	15.296	0.251	0.0004
15.296	0.591	0.0010	30.39	0.298	0.0002
30.390	0.657	0.0006	50.65	0.328	0.0002
50.650	0.695	0.0004			

[a]Standard uncertainties are $u(T_1)=0.8$ K, $u(V_1)=0.01$ mL, $u(V_2)=0.005$ mL, $u(P)=0.5$ kPa at 313 K

[b]Standard uncertainties are $u(T_1)=0.9$ K, $u(V_1)=0.01$ mL, $u(V_2)=0.005$ mL, $u(P)=0.5$ kPa at 363 K

Table 11 CO_2 solubility data in aqueous MEA/AMP/BEA blends

313.15 K[a]			363.15 Kb		
P_{CO_2}(kPa)	α (mol/mol)	$u(\alpha)$	P_{CO_2}(kPa)	α (mol/mol)	$u(\alpha)$
0.1 mol/L MEA + 1 mol/L AMP + 1 mol/L BEA					
8.104	0.637	0.0019	15.296	0.288	0.0004
15.296	0.669	0.0011	30.39	0.338	0.0003
30.390	0.732	0.0006	50.65	0.378	0.0002
50.650	0.789	0.0004			
0.3 mol/L MEA + 1 mol/L AMP + 1 mol/L BEA					
8.104	0.591	0.0017	15.296	0.299	0.0005
15.296	0.632	0.0010	30.39	0.341	0.0003
30.390	0.698	0.0006	50.65	0.381	0.0002
50.650	0.771	0.0004			
0.5 mol/L MEA + 1 mol/L AMP + 1 mol/L BEA					
8.104	0.587	0.0017	15.296	0.307	0.0005
15.296	0.632	0.0010	30.39	0.346	0.0003
30.390	0.695	0.0006	50.65	0.399	0.0002
50.650	0.731	0.0004			
0.1 mol/L MEA + 2 mol/L AMP + 2 mol/L BEA					
8.104	0.501	0.0017	15.296	0.251	0.0004
15.296	0.527	0.0010	30.39	0.269	0.0002
30.390	0.566	0.0006	50.65	0.307	0.0002
50.650	0.612	0.0004			
0.3 mol/L MEA + 2 mol/L AMP + 2 mol/L BEA					
8.104	0.489	0.0015	15.296	0.252	0.0004
15.296	0.516	0.0008	30.39	0.271	0.0002
30.390	0.543	0.0004	50.65	0.314	0.0002
50.650	0.589	0.0003			
0.5 mol/L MEA + 2 mol/L AMP + 2 mol/L BEA					
8.104	0.478	0.0014	15.296	0.257	0.0004
15.296	0.509	0.0008	30.39	0.287	0.0002
30.390	0.537	0.0004	50.65	0.326	0.0002
50.650	0.579	0.0004			

[a]Standard uncertainties are $u(T_1)=0.8$ K, $u(V_1)=0.01$ mL, $u(V_2)=0.005$ mL, $u(P)=0.5$ kPa at 313 K

[b]Standard uncertainties are $u(T_1)=0.9$ K, $u(V_1)=0.01$ mL, $u(V_2)=0.005$ mL, $u(P)=0.5$ kPa at 363 K

At 363 K, a relatively high increase in CO_2 solubility was observed when increasing the MEA concentration from 0.3 to 0.5 mol/L. In this case, it could be confirmed that MEA/BEA/AMP (0.3 + 2 + 2 mol/L) is the optimized ratio compared to other two ratios.

By considering the coordinative effect, Shi et al. (2021a, b) found that addition of MEA (0.1 to 0.5 mol/L) into the bi-solvent blends (2 mol/L BEA + 2 mol/L AMP) could improve the absorption mass transfer performance, which consequently causes the higher initial absorption rate compared to the bi-solvent without MEA. Besides, the addition of MEA at the specified ratio (MEA/RR′NH = 0.5/2) could potentially enhance the heat duty

Table 12 Equilibrium solubility of CO_2 in several aqueous amine blends

Amine type	Concentration	Sources	P_{CO_2}(kPa)	T (K)	$d(\text{Ln } P_{CO_2})/d(1/T)$
MEA-AMP-BEA	0.1–2-2 mol/L ($\alpha=0.6$)	Shi et al. (2021a, b)	13.50	298	−7479.1
		This work*	44.95	313	
	0.3–2-2 mol/L ($\alpha=0.58$)	Shi et al. (2021a, b)	13.50	298	−7824.3
		This work*	47.51	313	
	0.5–2-2 mol/L ($\alpha=0.57$)	Shi et al. (2021a, b)	13.50	298	−7859.4
		This work*	47.75	313	
MEA-AMP	0.1–2 mol/L ($\alpha=0.79$[a])	This work	15.30	298	−5122.5[b]
		This work*	34.87	313	
	0.3–2 mol/L ($\alpha=0.76$[a])	This work	15.30	298	−5819.1[b]
		This work*	38.99	313	
	0.5–2 mol/L ($\alpha=0.73$[a])	This work	15.30	298	−5538.6[b]
		This work*	37.28	313	
MEA-BEA	0.1–2 mol/L ($\alpha=0.70$[a])	This work	15.30	298	−5866.1[b]
		This work*	38.81	313	
	0.3–2 mol/L ($\alpha=0.69$[a])	This work	15.30	298	−6069.2[b]
		This work*	40.60	313	
	0.5–2 mol/L ($\alpha=0.67$[a])	This work	15.30	298	−6129.8[b]
		This work*	41.00	313	

*Estimated from the proposed experimental data (from Tables 9, 10, and 11) via exponential nonlinear relations

[a]Standard uncertainties are $u(T_1)=0.75$ K, $u(V_1)=0.01$ mL, $u(V_2)=0.005$ mL, $u(P)=0.5$ kPa at 298 K

[b]With accuracy ± 3%

reduction by boosting amine regeneration and CO_2 production. From this study, the concentration of AMP/BEA plays a key role at 363 K. In addition, the more unstable carbamate produced from AMP could significantly lower the negative impact of the absorption capacity of MEA, which is beneficial for desorption. It is also reported by Narku-Tetteh et al. (2017a, b) that the equilibrium CO_2 solubility has a positive relationship with the alkyl chain length of the secondary amines. BEA is a secondary amine with a long-chain alkyl group, which increases the basicity of the solvent by converting the electrons from the nitrogen ion to the alkyl group. BEA thus exhibited excellent reactivity when being blended with AMP and MEA, particularly advantageous at 313 K. Furthermore, 4 mol/L BEA/AMP is obviously more viscous than 2 mol/L BEA/AMP so the mass transfer limitation increases as the solvent viscosity increases (Narku-Tetteh et al. 2017a, b). The further work is worthy to obtain the direct effect of the solvent viscosity on the CO_2 solubility. Also, the varied ratio of AMP/BEA is another considering factor for the further work.

Heat of CO_2 absorption

In this work, the equilibrium CO_2 solubility data at 298 K were obtained from the published data sets (Shi et al. 2021a, b) and the new experimental data. To determine the term of $\frac{d(\text{Ln}(P_{CO_2}))}{d(\frac{1}{T})}$, it is necessary to keep the CO_2 loading as a constant as shown in Table 12. The estimated heat of CO_2 absorption in several solvent blends was eventually summarized as shown in Table 13, which displayed the effect of MEA on the heat of CO_2 absorption. Adding MEA can potentially increase the absorption heat of CO_2. It can be attributed by the structural characteristic. Narku-Tetteh et al. (2017a, b) reported that all the side chain (hindered) amines exhibited higher heat of CO_2 absorption than the straight chain (unhindered) amines. A higher amount of CO_2 absorbed in hindered amines causes more heat released compared to their straight chain analogues. Moreover, the increase in MEA in the solvents of MEA/AMP and MEA/AMP/BEA exhibited more stable carbamate which is formed when MEA reacts with CO_2 and has a higher enthalpy of reaction. Considering the AMP-CO_2-H_2O system, the steric hindrance of the methyl group causes the low stability of AMP carbamate (Muchan et al. 2017), which increases the rate of bicarbonate formation through carbamate hydrolysis. According to the work of Muchan et al. (2017), the formation of bicarbonate is an endothermic reaction while the carbamate formation is an exothermic reaction, which is the main reason for more stable carbamate formation leading to a higher ΔH_a. Therefore, it was

Table 13 CO_2 absorption heat in various aqueous solvent blends at temperature range of 298–313 K

Amine type	Concentration	ΔH_a [a] (kJ/mol)
MEA-AMP-BEA	0.1–2-2 mol/L (α = 0.6)	− 62.18
	0.3–2-2 mol/L (α = 0.58)	− 65.12
	0.5–2-2 mol/L (α = 0.57)	− 65.19
MEA-AMP	0.1–2 mol/L (α = 0.79)	− 42.58
	0.3–2 mol/L (α = 0.76)	− 48.25
	0.5–2 mol/L (α = 0.73)	− 45.97
MEA-BEA	0.1–2 mol/L (α = 0.70)	− 48.69
	0.3–2 mol/L (α = 0.69)	− 50.36
	0.5–2 mol/L (α = 0.67)	− 50.96

[a]With accuracy ± 3%

found that ΔH_a is strongly affected by CO_2 loading, rate of carbamate formation, rate of bicarbonate formation, and amount of free amine in the solvent. The heat of CO_2 absorption is directly related to desorption heat, which is an important parameter to estimate the energy requirements of the amine desorption process. Combined with the proposed equilibrium solubility data in the previous sections, it could be summarized that the effect of MEA (0.1–0.5 mol/L) on the CO_2 solubility and the heat of

Table 14 Prediction accuracy of the ANN and KE models

T (K)	Bi-solvent		Tri-solvent	
	KE	ANN	KE	ANN
313	4.67	3.25	3.69	5.94
363	12.24	6.49	12.54	10.45
AVG	8.43	4.87	8.11	8.19

CO_2 absorption in aqueous BEA exhibited the lowest impact, which is beneficial for both absorption and desorption processes.

The possible errors of absorption heat estimation can be analyzed as two perspectives. First, the calculations of the absorption heat were on the basis of CO_2 loading distributed at two temperatures. The uncertainties of the solubility data led to a maximum 3% of possible error. Second, the estimated absorption heat using Gibbs–Helmholtz equation could have a slight difference compared to the experimental result via the calorimeter. Liu et al. (2017a, b) investigated the absorption heat of MEA, DEA, and MDEA by using two methods. Despite that the estimated heats of CO_2 absorption based on the Gibbs–Helmholtz equation were in good agreement with

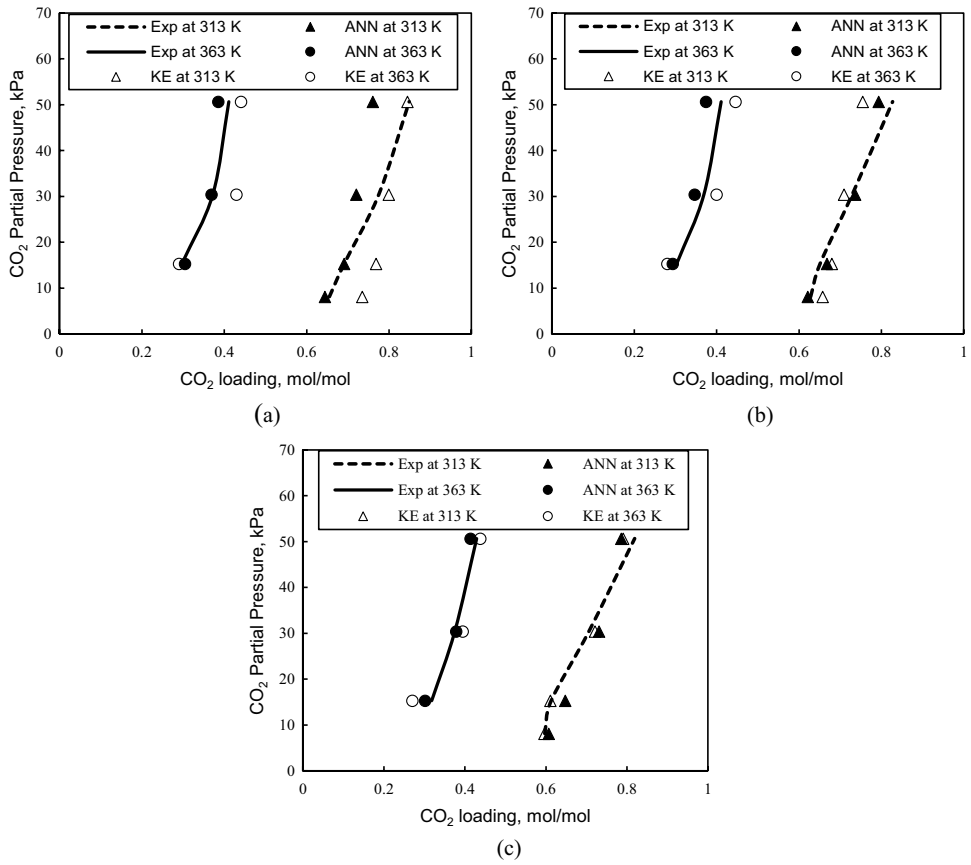

Fig. 5 ANN predictions vs experimental results (MEA/AMP). **a** 0.1 mol/L MEA + 2 mol/L AMP. **b** 0.3 mol/L MEA + 2 mol/L AMP. **c** 0.5 mol/L MEA + 2 mol/L AMP

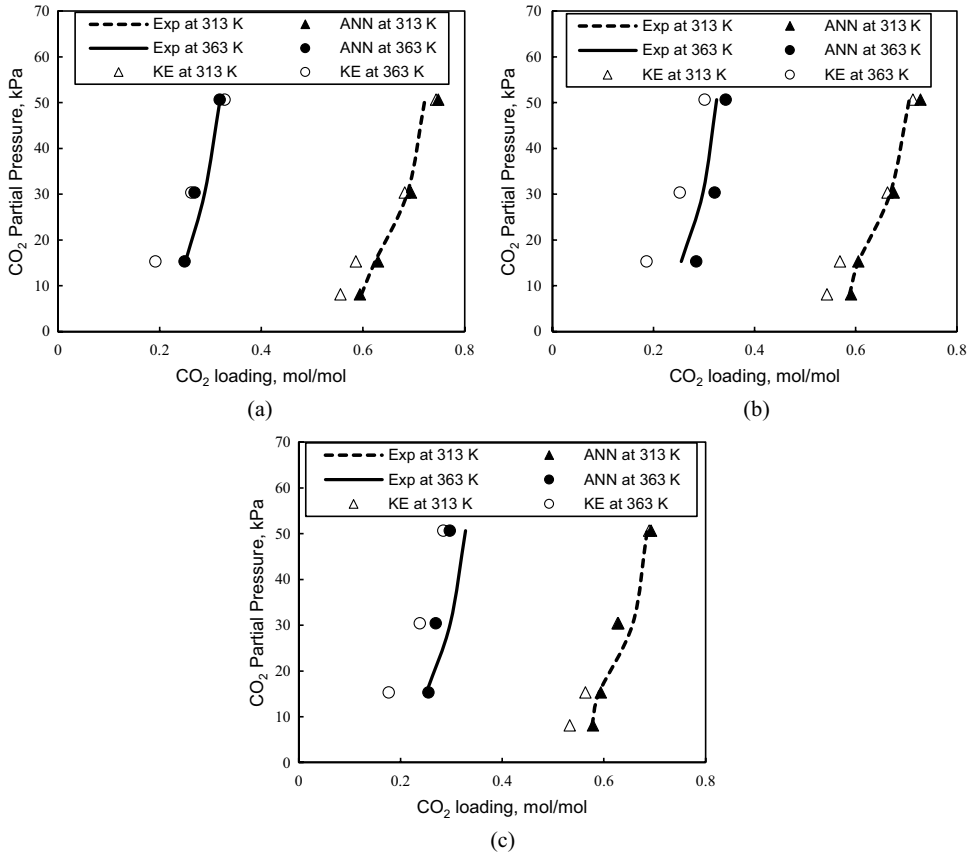

Fig. 6 ANN predictions vs experimental results (MEA/BEA). **a** 0.1 mol/L MEA + 2 mol/L BEA. **b** 0.3 mol/L MEA + 2 mol/L BEA. **c** 0.5 mol/L MEA + 2 mol/L BEA

the experimental results, the comparisons still showed 3% to 11% of differences. Typically, it is usually difficult to specify the exact deviation of the estimated absorption heat compared to the experimental results. The deviation mostly depends on the operating conditions and the solvent. However, both methods tended to have a consistent trend of the change in terms of CO_2 absorption heat.

Modeling approach

ANN and KE model

The experimental data were then correlated with the predictions using two model approaches. Both two models can predict the solubility of CO_2 with great agreement with experimental data as shown in Table 14. For the predictions of bi-solvent, the %AAD using ANN (4.87%) is significantly lower than KE modeling (8.43%), while the KE model contributes a slightly lower %AAD (8.11%) than ANN (8.19%) when predicting the solubility of CO_2 in tri-solvent. The prediction accuracy of two models was both reduced at elevated temperature. Typically, the input variables that have weak predictive power could negatively affect the accuracy of ANN prediction. The predictive power of the input variable is generally defined by the prediction objectives. To improve the prediction accuracy of ANN for tri-solvent, the most direct strategy is to re-train the model with the experimental data using tri-solvent. Unfortunately, the studies related to BEA are extremely novel, and this work is the first study for the investigations of the solubility in aqueous MEA/AMP/BEA. Therefore, it becomes one major limitation for optimizing the ANN model. However, it should be mentioned that there are two strategies that can be applied to improve the accuracy of the prediction based on a limited data set, including the weighting management and the capacity management of the nonlinear network. There are some other limitations that should be clearly addressed: (i) though the ANN model gives a reasonable solution, it does not provide a detailed reason or procedure to show why and how the results generated. For the new users without any experience on this research area, they may query the results. (ii) There is no uniform rule to determine the most appropriate network structure and appropriate amount of input data. (iii) It is difficult to see the exact reason of error, because all

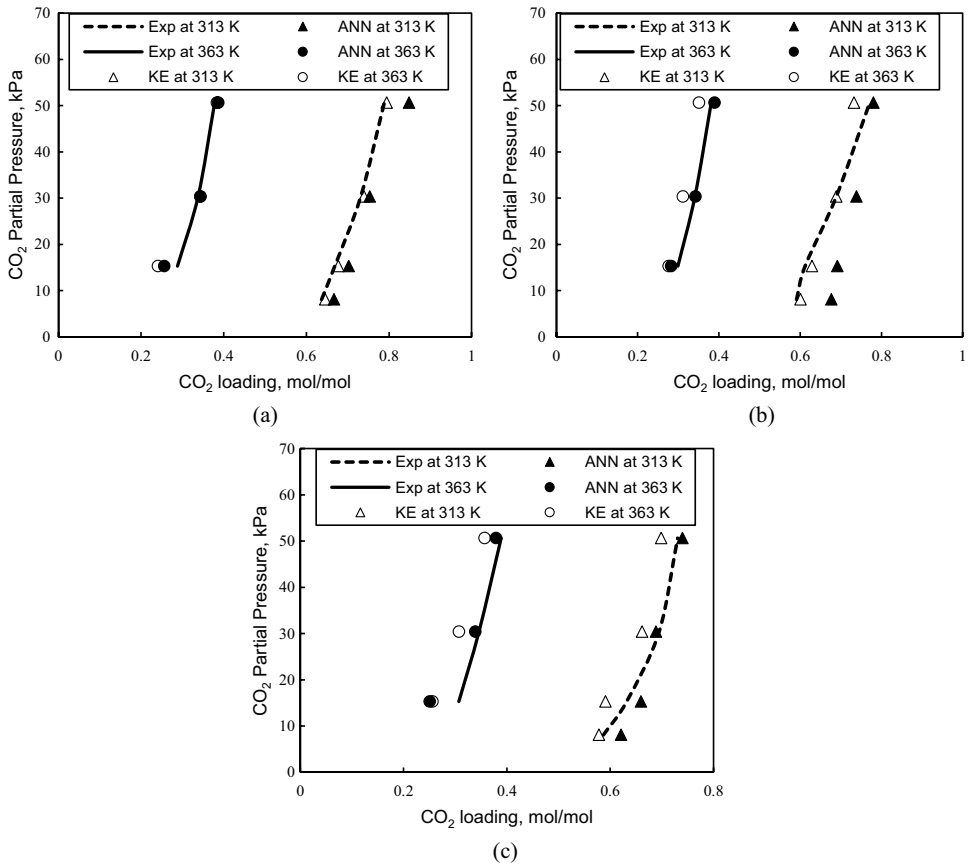

Fig. 7 ANN predictions vs experimental results (MEA/AMP/BEA 2.1 ~ 2.5 mol/L). **a** 0.1 mol/L MEA + 1 mol/L AMP + 1 mol/L BEA. **b** 0.3 mol/L MEA + 1 mol/L AMP + 1 mol/L BEA. **c** 0.5 mol/L MEA + 1 mol/L AMP + 1 mol/L BEA

training and testing data should be numerically pretreated first. Thus, all the outputs are generated and translated into numerical values. The above limitations can potentially increase the uncertainties of using ANN. So far, the most simple and effective method to reduce the negative impact is to optimize the network through error analysis.

The comparisons of each solvent are presented graphically in Figs. 5, 6, 7, and 8. The predicted CO_2 solubility shows good agreement with the experimental results. The relatively high deviation regions are observed in Figs. 7 and 8. This demonstrates that the ANN model has greater learning ability to predict the CO_2 solubility in bi-solvent than that of tri-solvent because of the reduced complexity. A similar trend was also discussed by Li et al. (2021) showing that they developed two model structures for bi-solvent and tri-solvent, respectively. Their results indicated that it is an efficient strategy to improve the prediction accuracy based on the identical training algorithm due to the greater learning capacity. It is true that the intrinsic mechanisms of tri-solvent blends are normally more complicated than single solvent and bi-solvents. However, it is the major superiority of the ANN model. The model of this work was developed based on the CO_2 solubility data in several single solvents and amine blends. Despite that, the selection of the training data needs to be carefully screened through detailed error analysis. Once the data sets are well-prepared, the learning ability and the computations of the CO_2 solubility are convenient and fast. In general, though the operating conditions of the CO_2 solubility are varied from different studies, ANN is able to extract the most relevant data with excellent learning flexibility through the given network and it is also a time-saving prediction tool with great efficiency based on the given database. In addition, if the further network needs to predict CO_2 solubility at a wider range of operating conditions, the network then would be relatively more complicated, ANNs can also be properly managed by the settings of its learning algorithm parameters and the weights of the variables. These advantages of ANN help the predictions of CO_2 solubility more closely to the real experimental data.

The predicted results and experimental results are displayed in Fig. 9. The correlation coefficient was found as 0.9807, which confirmed that the proposed ANN architecture provided excellent prediction ability and could be used for further predictions.

ANN and other thermodynamics models

Vapor–liquid equilibria (VLE) characterizations of alkanomine-CO_2-water systems are widely studied

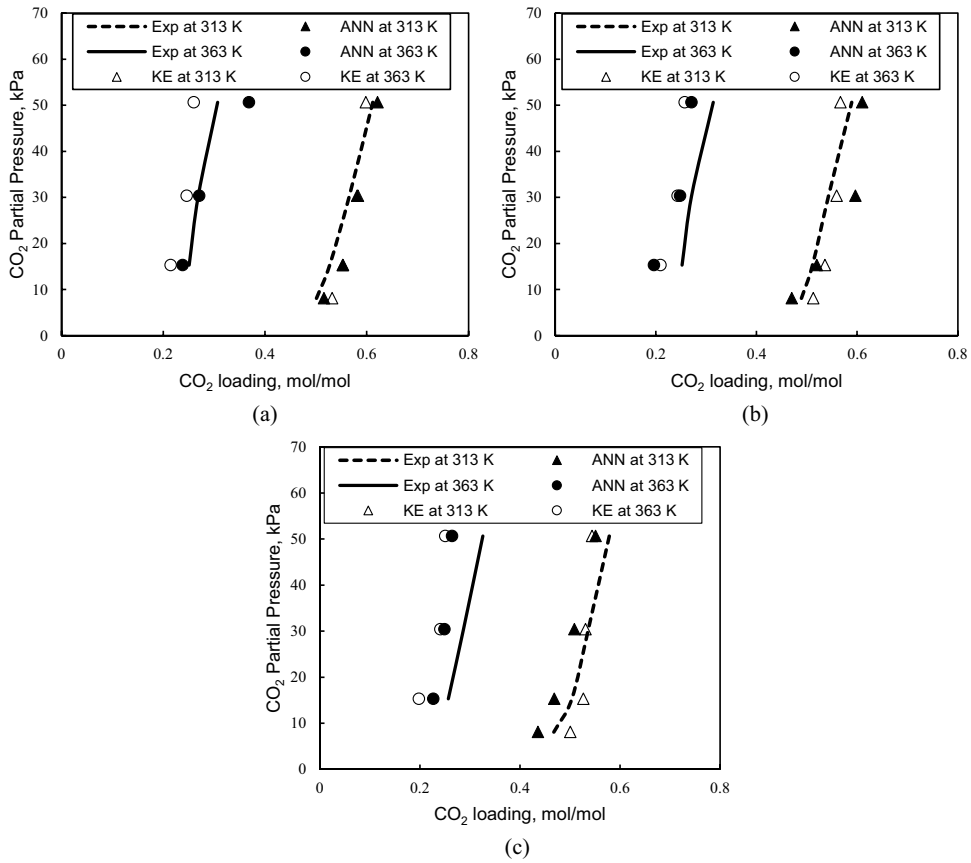

Fig. 8 ANN predictions vs experimental results (MEA/AMP/BEA 4.1 ~ 4.5 mol/L). **a** 0.1 mol/L MEA + 2 mol/L AMP + 2 mol/L BEA. **b** 0.3 mol/L MEA + 2 mol/L AMP + 2 mol/L BEA. **c** 0.5 mol/L MEA + 2 mol/L AMP + 2 mol/L BEA

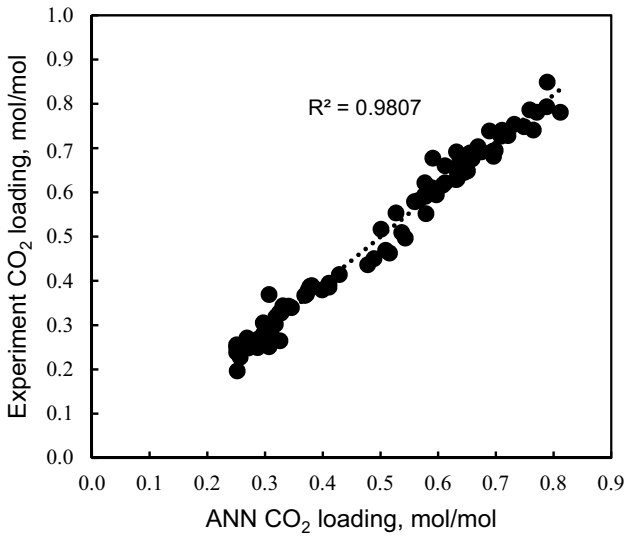

Fig. 9 The correlation coefficient

through the SAFT. In general, SAFT can be categorized as an association theory related to the perturbation theories by determining the total energy of hydrogen bonding via statistical mechanics (Yazdi et al. 2020). The schematic representation of the SAFT theory was discussed by Yazdi et al. (2020) that divided into four parts: first, molecules are formed by the addition of equal-sized spherical segments; second, the dispersion force drives the formed molecules that gain specific interaction sites at certain positions; third is the formation of molecule chains; and lastly, hydrogen bonding between the chains is associated with attractive interaction to form a complex structure. Compared to other empirical equations, the existence of a clear molecule drives the SAFT Equation of State (EOS) to be more beneficial for complex fluid modeling (Yazdi et al. 2020).

PC-SAFT EOS was applied to predict the VLE properties of MEA by Baygi and Pahlavanzadeh. (2015). It was expressed in terms of free Helmholtz energy (Gross and Sadowski 2001), which is a combination of contribution in three terms: (1) the hard-chain reference fluid consists of spherical segments Helmholtz energy; (2) the dispersive interactions to the Helmholtz energy; and (3) the short-range association hydrogen bonding interactions among segments in the free Helmholtz energy. SAFT-HR EOS was firstly introduced by Huang and Radosz (1990), who investigated the free Helmholtz energy from the contributions of the hard sphere, dispersion interaction, chain-forming bonds, and association terms. Over the past three decades, Najafloo and

Zarei (2018) were the first group of researchers to use the SAFT-HR EOS for the estimation of VLE properties of the MEA + CO_2 + water system; they eventually reported a comparison between capabilities of SAFT-HR EOS and PC-SAFT EOS in prediction of the CO_2 solubility in aqueous MEA solvent. In their study, a set of prediction of equilibrium CO_2 solubility was carried out in a temperature range of 298 to 443 K and a pressure range of 0.0012 to 19,954 kPa. However, due to the limited range of the input data of the present ANN model, the comparison of predictions between ANN and SAFT EOS in this study was implemented at a temperature range from 313 to 393 K as shown in Table 15.

It is well known that the main limitation of using ANN highly relies on the training data. The ANN model would not be able to predict the CO_2 solubility data accurately once the given input data are inefficient. From Table 15, the %AAD of using ANN is greatly lower than the other two models while the estimation range (pressure, temperature, and concentration of amine) of sample data is fully covered in the trained dataset. However, the present ANN model cannot predict the data from Dawodu and Meisen (1994) very well because their experiments were completed at high pressures. Although Najafloo and Zarei (2018) summarized that SAFT-HR EOS is more accurate from a greater comprehensive perspective compared to PC-SAFT EOS, ANN is still more accurate than both two SAFT EOSs when predicting the solubility of CO_2 at low pressures. There are also some significant benefits that appeared during the study. For instance, ANN could directly predict CO_2 solubility in the blended amine system in a short time. However, the main limitation of the present ANN model from this work is its limited prediction range, and it could not accurately predict CO_2 solubility at high pressures. The further research can update the training dataset if the requirement of the model is used to predict the CO_2 solubility at wider range of temperature and pressure.

Conclusions

The experiments of this work were conducted at temperatures of 313 and 363 K and CO_2 partial pressure up to 50.66 kPa. This study aims to investigate the CO_2 solubility in several amine blends with specific concentration, including MEA + AMP (0.1, 0.3, 0.5 mol/L + 2 mol/L), MEA + BEA (0.1, 0.3, 0.5 mol/L + 2 mol/L), and MEA + AMP + BEA (0.1, 0.3, 0.5 mol/L + 1, 2 mol/L + 1, 2 mol/L). To sum up everything that has been stated so far, MEA could potentially reduce the absorption capacity at 313 K for the solvents mentioned above, while MEA could also slightly increase the absorption capacity at high temperature conditions (363 K). It was also observed that the effect of adding additional MEA into the aqueous solvent on the CO_2 solubility could depend on several factors, including amine type, total amine concentration, amine concentration ratio, temperature, and CO_2 partial pressure. Considering the heat of CO_2 solubility in the tested solvents, the impact of increasing MEA into the aqueous BEA solvent is less significant compared to other solvents, which is potentially more beneficial for amine desorption. The heat of CO_2 solubility can also be affected by several parameters, including CO_2 loading, amine type, and CO_2 solubility. For a comprehensive study, it is essential to have further relevant investigations, such as viscosity, reaction kinetics and solvent stability. For modeling, an ANN model with two hidden layers consisting of 10 and 4 neurons was developed using the LM algorithm and tansig nonlinear transmission function. The advantages and limitations of the ANN method were all discussed in the front section by comparing it with the typical thermodynamics model. The predictions from the ANN model were in excellent agreement with the experimental results with a low %AAD of 4.66%.

Nomenclature P_{CO_2}: CO_2 partial pressure, kPa; T: Operating temperature, K or °C; X: The overall concentration of the amine in the solvent, wt.%; X_{MEA}: Weight fraction of MEA, wt.%; X_{AMP}: Weight fraction

Table 15 Prediction accuracy of ANN and SAFT EOS

Sources	T (K)	P_{CO_2}(kPa)	MEA weight fraction (wt.%)	Data points	%AAD		
					SAFT-HR[a]	PC-SAFT[b]	ANN[*]
Austgen et al. (1991)	313–353	0.093–228	15	8	12.35	11.97	7.97
Jane and Li. (1997)	353	3.57–121.8	15	7	27.33	30.91	9.21
Jones et al. (1951)	313–393	1.4–374	15	50	19.71	26.17	25.74
Dawodu and Meisen (1994)	373	455–3863	25	5	26.80	17.05	50.11
Park et al. (2002)	313	2.59–2189.1	10–15.3	13	37.59	50.65	27.87
Isaacs et al. (1980)	353–373	0.0066–1.75	15	16	27.45	22.66	9.58

[a]Gross et al. (2001)

[b]Yazdi et al. (2020)

[*]This work

of AMP, wt.%; X_{BEA}: Weight fraction of BEA, wt.%; MW_a: Apparent molecular weight, g/mol; MEA: Monoethanolamine; AMP: 2-Amino-2-methyl-1-propanol; BEA: 2-(Butylamino)ethanol; CO_2: Carbon dioxide; Y_i: The normalized training and testing data sets; x_i: The training and testing data sets; x_{min}: The minimum values of variable; x_{max}: The maximum values of variable; %AAD: The absolute average deviation, %; R^2: The correlation coefficient; MSE: The mean square errors; EXP: Exponential function; A: CO_2 loading, mol_{CO2}/mol_{amine}

Acknowledgements The generous support of the Natural Science and Engineering Research Council of Canada (NSERC) is gratefully acknowledged. The editorial help of Angel Charles is also gratefully acknowledged.

Author contribution Li T. and Yang C. conducted the research; Li T. wrote the paper; Li T. conducted the literature study; Sema T., Tantikhajorngosol P., Shi H., and Tontiwachwuthikul P. revised the paper.

Data availability Not applicable.

Declarations

Ethics approval Not applicable.

Consent to participate Not applicable.

Consent for publication Not applicable.

Competing interests The authors declare no competing interests.

References

Aronu UE, Gondal S, Hessen ET, Warberg TH, Hartono A, Hoff KA, Svendsen HF (2017) Solubility of CO_2 in 15,30,45 and 60 mas% MEA from 40 to 120°C and model representation using the extended UNIQUAC framework. Chem Eng Sci 66:6393–6406

Austgen DM, Rochelle GT, Chen CC (1991) Model of vapor-liquid equilibria for aqueous acid gas-alkanolamine systems. 2. Representation of hydrogen sulfide and carbon dioxide solubility in aqueous MDEA and carbon dioxide solubility in aqueous mixtures of MDEA with MEA or DEA. Ind Eng Chem Res 30(3):543–555

Baygi SF, Pahlavanzadeh H (2015) Application of the perturbed chain-SAFT equation of state for modeling CO_2 solubility in aqueous monoethanolamine solutions. Chem Eng Res Des 93:789–799

Chen G, Luo X, Zhang H, Fu K, Liang Z, Rongwong W (2015) Artificial neural network models for the prediction of CO_2 solubility in aqueous amine solutions. Int J Greenh Gas Control 39:174–184

Choi BK, Kim SM, Lee JS, Park YC, Chun DH, Shin HY, Sung HJ, Min BM, Moon JH (2020) Effect of blending ratio and temperature on CO_2 solubility in blended aqueous solution of monoethanolamine and 2-amino-2-methyl-propanol: experimental and modeling study using the electrolyte nonrandom two-liquid model. ACS Omega 5(44):28738–28748

Coker J, Afari DB, Tetteh J, Idem R (2017) Mass-transfer studies of solid-base catalyst-aided CO_2 absorption and solid-acid catalyst-aided CO_2 desorption for CO_2 capture in a pilot plant using aqueous solutions of MEA and blends of MEA-MDEA and BEA-AMP. Clean Energy 3:263–277

Dawodu OF, Meisen A (1994) Solubility of carbon dioxide in aqueous mixtures of alkanolamines. J Chem Eng Data 39(3):548–552

Edwards TJ, Maurer G, Newman J (1978) Vapor-liquid equilibria in multicomponent aqueous solutions of volatile weak electrolytes. ALChE J 24(6):966–976

Fu K, Chen G, Sema T, Zhang X, Liang Z, Idem R, Tontiwachwuthikul P (2013) Experimental study on mass transfer and prediction using artificial neural network for CO_2 absorption into aqueous DETA. Chem. Eng. Sci 100:195–202

Golzar K, Modarress H, Amjad-Iranagh S (2016) Evaluation of density, viscosity, surface tension and CO_2 solubility for single, binary and ternary aqueous solutions of MDEA, PZ and 12 common ILs by using artificial neural network (ANN) technique. Int J Greenh Gas Control 53:187–197

Gross J, Sadowski G (2001) Perturbed-chain SAFT: An equation of state based on a perturbation theory for chain molecules. Ind Eng Chem Res 40(4):1244–1260

Haji-Sulaiman MZ, Aroua MK, Benamor A (1998) Analysis of equilibrium data of CO_2 in aqueous solutions of diethanolamine (DEA), methyldiethanolamine (MDEA) and their mixtures using the modified Kent Eisenberg model. Trans IchemE 76:961–868

Hamborg ES, Versteeg GF (2009) Dissociation constants and thermodynamic properties of amines and alkanolamines from (293 to 353) K.J. Chem Eng Data 54(4):1318–1328

Hamzehie ME, Mazinani S, Davardoost F, Mokhtare A, Najibi H, Van der Bruggen B, Darvishmanesh S (2014) Developing a feed forward multilayer neural network model for prediction of CO_2 solubility in blended aqueous amine solutions. J Nat Gas Sci Eng 21:19–25

He J, Xu X, Gui X (2021) New vapor-liquid phase equilibrium data of CO_2 in several heavy n-alanes at high pressures. J Chem Eng Data 66(4):1600–1610

Hu W, Chakma AA (1990) modeling of equilibrium solubility of CO_2 and H_2S in aqueous amino methyl propanol (AMP) solutions. Chem Eng Commun 94(1):53–61

Huang SH, Radosz M (1990) Equation of state for small, large, polydisperse, and associating molecules. Ind Eng Chem Res 29(11):2284–2294

Hwang SJ, Kim H, Lee KS (2016) Prediction of VLE for aqueous blended amines using VLE models of single amines. Int J Greenh Gas Control 49:250–258

Hwang SJ, Kim J, Kim H, Lee KS (2017) Solubility of carbon dioxide in aqueous solutions of three secondary amines: 2-(butylamino)ethanol, 2-(isopropylamino)ethanol, and 2-(ethylamino) ethanol secondary alkanolamine solutions. J Chem Eng Data 62(8):2428–2435

International Energy Agency (2020) World Energy Outlook 2020 Part of World Energy Outlook., IEA, Paris

Isaacs EE, Otto FD, Mather AE (1980) Solubility of mixtures of hydrogen sulfide and carbon dioxide in a monoethanolamine solution at low partial pressures. J Chem Eng Data 25(2):118–120

Jane IS, Li M (1997) Solubilities of mixtures of carbon dioxide and hydrogen sulfide in water + diethanolamine +2-amino-2-methyl-1-propanol. J Chem Eng Data 42:98–105

Jones JH, Froning HR, Claytor EE (1951) Solubility of acidic gases in aqueous monoethanolamine. J Chem Eng Data 4:85–92

Kent RL, Eisenberg B (1976) Better data for amine treating. Hydrocarb Process 1:60–165

Kundu M, Mandal B, Bandyopadhyay S (2003) Vapour -liquid equilibria of CO_2 in aqueous solutions of 2-amino-2-methyl-1-propanol. J Chem Eng Data 48(4):789–796

Li M, Chang BC (1995) Solubility of mixtures of carbon dioxide and hydrogen sulfide in water + monoethanolamine + 2-amino-2-mehtyl-1-propanol. J Chem Eng Data 40:328–331

Li M, Shen K (1993) Calculation of equilibrium solubility of carbon dioxide in aqueous mixtures of monoethanolamine with methyldiethanolamine. Fluid Phase Equilib 85:129–140

Li C, Liu H, Xiao M, Luo X, Gao H, Liang Z (2017) Thermodynamics and ANN models for predication of the equilibrium CO_2 solubility in aqueous 3-dimethylamino-1-propanol solution. Int J Greenh Gas Control 63:77–85

Li T, Tantikhajorngosol P, Yang C, Tontiwachwuthikul P (2021) Experimental investigations and developing multilayer neural network models for prediction of CO_2 solubility in aqueous MDEA/PZ and MEA/MDEA/PZ blends. Greenh Gases: Sci Technol 11(4):712–733

Liu H, Li M, Idem R, Tontiwachwuthikul P, Liang Z (2017) Analysis of solubility, absorption heat and kinetics of CO_2 absorption into 1-(2-hydroxyethyl)pyrrolidine solvent. Chem Eng Sci 162:120–130

Liu H, Xiao M, Tontiwachwuthikul P, Liang Z (2017) A novel model for correlation and prediction of the equilibrium CO_2 solubility in seven tertiary solvents. Energy Procedia 105:4476–4481

Liu H, Chan C, Tontiwachwuthikul P, Idem R (2019) Analysis of CO_2 equilibrium solubility of seven tertiary amine solvents using thermodynamic and ANN models. Fuel 249:61–72

Mazinani S, Samsami A, Jahanmiri A, Sardarian A (2011) Solubility (at low partial pressures), density, viscosity and corrosion rate of carbon dioxide in blend solutions of monoethanolamine (MEA) and sodium glycinate (SG). J Chem Eng Data 56(7):3163–3168

Mondal BK, Bandyopadhyay S, Samanta AN (2017) Experimental measurement and Kent-Eisenberg modelling of CO_2 solubility in aqueous mixture of 2-amino-2-methyl-1-propanol and hexamethylenediamine. Fluid Phase Equilib 437:118–126

Muchan P, Saiwan C, Narku-Tetteh J, Idem R, Supap T, Tontiwachwuthikul P (2017) Screening tests of aqueous alkanolamine solutions based on primary secondary and tertiary structure for blended aqueous amine solution selection in post combustion CO_2 capture. Chem Eng Sci 170:574–582

Murshid G, Garg S, Ali A, Maqsood K, See T (2020) An experimental and modeling to investigate CO_2 solubility in blended aqueous solutions of 2-amino-2-hydroxymethyl-1, 3-propanediol (AHPD) and piperazine (PZ). Cleaner Eng Technol 1:100004

Najafloo A, Zarei S (2018) Modeling solubility of CO_2 in aqueous monoethanolamine (MEA) solution using SAFT-HR equation of state. Fluid Phase Equilib 456:25–32

Narku-Tetteh J, Muchan P, Idem R (2017) Effect of alkanol chain length of primary alkanolamines and alkyl chain length of secondary and tertiary alkanolamines on their CO_2 capture activities. Sep Purif Technol 187:453–467

Narku-Tetteh J, Muchan P, Saiwan C, Supap T, Idem R (2017) Selection of components for formation of amine blends for post combustion CO_2 capture based on the side chain structure of primary, secondary, and tertiary amines. Chem Eng Sci 170:542–560

Pahlavanzadeh H, Nourani S, Seber M (2011) Experimental analysis and modeling of CO_2 solubility in AMP (2-amino-2-methyl-1-propanol) at low CO_2 partial pressure using the models of Deshmukh-Mather and the artificial neural network. J Chem Thermodyn 43(26):1775–1783

Park JY, Yoon SJ, Lee H, Yoon JH, Shim JG, Lee JK, Min BY, Eum HM, Kang MC (2002) Solubility of carbon dioxide in aqueous solutions of 2-amino-2-ethyl-1,3-propanediol. Fluid Phase Equilib 202(2):359–366

Ping T, Dong Y, Shen S (2020) Energy-efficient CO_2 capture using nonaqueous absorbents of secondary alkanolamines with a 2-butoxyethanol cosolvent. ACS Sustainable Chem Eng 8(49):18071–18082

Portugal AF, Sousa JM, Magalhaes FD, Mendes A (2009) Solubility of carbon dioxide in aqueous solutions of amino acid salts. Chem. Eng. Sci 64:1993–2002

Rumpf B, Maurer G (1993) An experimental and theoretical investigation on the solubility of carbon dioxide in aqueous solutions of strong electrolytes. Ber Bunsen-Ges Phys Chem 97:85–97

Shen KP, Li MH (1992) Solubility of carbon dioxide in aqueous mixtures of monoethanolamine with methyldiethanolamine. J Chem Eng Data 37(1):96–100

Shi H, Cui M, Fu J, Dai W, Huang M, Han J, Quan L, Tontiwachwuthikul P, Liang Z (2021) Application of "coordinative effect" into tri-solvent MEA+BEA+AMP blends of concentrations of 0.1+2+2~0.5+2+2mol/L with absorption desorption and mass transfer analyses. Int J Greenh Gas Control 107:103267

Shi H, Feng H, Yang X, Zou T, Tontiwachwuthikul P, Jiang L (2021b) Study of "coordinative effect" within bi-blended amine MEA+AMP and MEA+BEA at 0.1+2–0.5+2 mol/L with absorption-desorption parameter analyses. Asia-Pac J Chem Eng 16(4)

Silkenbaumer D, Rumpt B, Lichtenthaler RN (1998) Solubility of carbon dioxide in aqueous solutions of 2-amino-2-methyl-1-propanol and n-methyldiethanolamine and their mixtures in the temperature range from 313 to 353K and pressure up to 2.7 Mpa. Ind Eng Chem Res 37(8):3133–3141

Singh P, Brilman DWF, Groeneveld MJ (2011) Evaluation of CO_2 solubility in potential aqueous amine-based solvents at low CO_2 partial pressure. Int J Greenh Gas Control 5(1):61–68

Sipocz N, Tobiesen FA, Assadi M (2016) The use of artificial neural network models for CO_2 capture plants. Appl Energy 88(7):2368–2376

Teng TT, Mather AE (1990) Solubility of CO_2 in an AMP solution. J Chem Eng Data 35:410–411

Tong D, Maitland C, Trusler M (2013) Fennell, P.S. Solubility of carbon dioxide in aqueous blends of 2-amino-2-methyl-1-propanol and piperazine. Chem Eng Sci 101:851–864

Tontiwachwuthikul P, Melsen A, Lim CL (1991) Solubility of CO_2 in 2-amino-2-methyl-1-propanol solutions. J Chem Eng Data 36(1):130–133

Xu S, Wang YW, Otto FD, Mather AE (1992) Representation of the equilibrium solubility properties of CO_2 with aqueous solutions of 2-amino-2-methyl-1-propanol. Chem Eng Process 31(1):7–12

Yazdi A, Najafloo A, Sakhaeinia H (2020) A method for thermodynamic modeling of H_2S solubility using PC-SAFT equation of state based on a ternary solution of water, methyldiethanolamine and hydrogen sulfide. J Molecular Liq 299:112113